1-1-1982

Neurobiological investigation of the pretectal region of the leopard frog, Rana pipiens.

Antony M. Grigonis
University of Massachusetts Amherst

Neurobiological Investigation of the Pretectal Region of the Leopard Frog, *Rana pipiens*

A Dissertation Presented

By

ANTONY M. GRIGONIS

Submitted to the Graduate School of the
University of Massachusetts in partial fulfillment
of the requirements for the degree of

DOCTOR OF PHILOSOPHY

September, 1982

Psychology Department

NEUROBIOLOGICAL INVESTIGATION OF THE PRETECTAL REGION OF THE LEOPARD FROG, RANA PIPIENS

A Dissertation Presented

By

ANTONY M. GRIGONIS

Approved as to style and content by:

Dr. Katherine V. Fite,
Chairperson of Committee

Dr. Gordon A. Wyse, Member

Dr. Stephen A. George, Member

Dr. Daniel R. Anderson, Member

Dr. Bonnie R. Strickland
Chairperson of Psychology

ACKNOWLEDGEMENT

I would especially like to thank my advisor, Dr. Katherine V. Fite, for providing me with an ideal balance between guidance and independence throughout the course of this dissertation. I would also like to thank the other members of my committee, Dr. Gordon Wyse, Dr. Stephen George, and Dr. Daniel Anderson, for their helpful suggestions and understanding during this work. A special thanks is extended to Lynn Bengston, for her expert histological help and advice, in addition to keeping my spirits high. I would also like to thank Neil Montgomery for his expert help in the anatomical analysis. Also, a note of thanks is extended to Jasmine Dali for her patience in typing, and to Jack Delmond for helping with the preparation of this manuscript.

A special note of thanks goes to all of my friends who helped me to take this work in stride.

This dissertation is dedicated to my mother and late father, for their confidence and support throughout my educational career leading to this degree.

ABSTRACT

Neurobiological Investigation of the Pretectal Region of the Leopard Frog, Rana pipiens

September, 1982

Antony M. Grigonis, B.S., Lehigh University

M.A., Adelphi University

Ph.D., University of Massachusetts

Directed by: Professor Katherine V. Fite

The neuroanatomical connections of the large-celled pretectal nucleus (LcPt) with other brain regions were determined through the retrograde and anterograde transport of horseradish peroxidase (HRP) following injection into LcPt. In addition, response properties of single units in the pretectal region were investigated using glass-coated, Woods-metal-filled micropipettes. Particular emphasis was placed on the response to stimuli which produce optokinetic nystagmus (OKN), since previous studies have inplicated the pretectal region as a neural correlate of OKN (Cochran, et al., 1980; Katte and Hoffmann, 1980; Montgomery, et al., in press).

The retinal afferents to LcPt originate from ganglion cells in the central portion of the retina. Other afferents to LcPt were found to originate from the optic tectum, the nucleus of the basal optic root (nBOR), the nucleus of the posterior commissure, and the anterior thalamic nucleus rotundus. In addition, two cell groups

outside LcPt send dendrites into the nucleus, including the ventral division of the posterior thalamic nucleus, and the region of pretectal gray. Efferents from LcPt travel to the peri-nBOR region, the anterior and caudolateral optic tectum, and the region superficial to the abducens nucleus (nVI). Cells in the ventral division of the posterior thalamic nucleus post-synaptic to LcPt were observed projecting to nVI.

Two types of unit responses to a moving OKN stimulus were observed in the pretectal region; transient responses to the onset or offset of OKN stimulation, and sustained or patterned responses which change during the presentation of a moving OKN stimulus. Several spontaneously active units in the pretectal gray region decreased their level of spontaneous activity during OKN stimulus movement for specific stimulus velocities. An inhibitory role in OKN processing for the pretectal gray region was suggested on the basis of these extracellular response properties as well as recent ablation studies (Fite, unpublished data). Only a small percentage of units were directionally-selective to OKN stimulus movement. The small number of directionally-selective units observed in the present study were presumed due to either the small sample size or to the use of criteria other than spontaneous activity for the encounter of a visually-responsive pretectal unit.

The present study has demonstrated that a high degree of anatomical complexity exists in the frog pretectal region. The large-celled pretectal nucleus appears to be interconnected with

several visuomotor and vestibular pathways. Also, the results of the present study support a homology between the frog LcPt and the mammalian nucleus of the optic tract, both in terms of the anatomical connections of this nucleus and its presumed role in the mediation of optokinetic nystagmus.

TABLE OF CONTENTS

LIST OF TABLES

LIST OF ILLUSTRATIONS

Figure

CHAPTER I

INTRODUCTION

Anurans, i.e., frogs and toads, represent one of the most successful orders of amphibians, since members can be found in every major region inhabitable by amphibians (Blair, 1976). The survival of anurans depends in part on vision--both prey-catching and predator avoidance in frogs and toads are considered primarily visually-guided behaviors. In fact, a large literature exists with regard to the anuran visual system (see Fite, 1976; Llinas and Precht, 1976 for review). Previous examination of the frog visual system, for example, has lead to two of the most widely used concepts in sensory physiology, the 'receptive-field' (Hartline, 1940), and 'feature-detection' (Lettvin, et al., 1959). More recently, the visual system of frogs and toads has been considered as a model which can provide insights into the mechanisms underlying basic visual processes (cf. Fite, 1976). Even though the amphibian brain does not possess a visual cortex, the anuran visual system can still be considered useful as a model of visual processes, in general, in part because

both amphibian and mammalian central nervous systems share similar first-order (retinofugal) visual projections. The analysis of neural correlates underlying visually-guided behavior is facilitated in anurans since their behavior is determined primarily by immediate stimulus configurations with little modification by learning and experience. The species of anuran under investigation in the present study, the leopard frog, Rana pipiens, is a behaviorally simple organism, and is abundant, inexpensive, and easy to maintain. In addition, leopard frogs represent a unique transition between aquatic and terrestrial vertebrates, since they reside in a true littoral habitat. Thus, new information on the anatomical and physiological mechanisms in the central visual system in Rana pipiens can be used as both a model for visual processing and as a basis of comparison with other more terrestrial or aquatic species.

Anurans, in general, show highly predictable species-specific visually-guided behaviors such as the barrier avoidance of toads (cf. Ewert, 1976), and the blue-preference of frogs (Muntz, 1962; Reuter and Virtanen, 1972; Fite, et al., 1978). One visually-guided behavior which is of particular interest in the present study, optokinetic nystagmus (OKN), is the reflexive compensatory motion of the head and eyes following the motion of an image across the retina. This response consists of pursuit or tracking movements of the head and eyes following the direction of a moving stimulus across the field of view, followed by an involuntary saccade in the opposite direction which enables the fixation of new contours just entering

the visual field. Optokinetic nystagmus has received recent attention in the study of the sensory-motor system of frogs (Lázár, 1973, Montgomery, et. al., 1981) as well as turtles (Hertzler and Hays, 1967), rabbits (Baarsma and Collewijn, 1974; Collewijn, 1975; Collewijn and Kleinschmidt, 1975; Dufossé et at., 1978; Simpson et al., 1979; Erickson, et al., 1980; Neverov, et al., 1980), cats (Carpenter, 1972; Thoden et al., 1979; Harris, et al., 1980; Hoffmann and Schoppmann, 1981; Montarolo, et al., 1981) and monkeys (Pasik and Pasik, 1964; Miles and Fuller, 1974; Pasik et al., 1977; Grüsser, et al., 1979; Hepp, et al., 1982).

Two basic conceptual frameworks have guided the study of the frog visual system since the pioneering work of Hartline (1940), and Lettvin, et al. (1959). A reductionistic approach implies a detailed analysis of a mechanism or system such as a brain, without regard to the overall functional significance of the components being examined. An integrative approach, on the other hand, refers to the analysis of components of a mechanism only as they relate to a specific function of that system. More loosely applied here, these concepts refer to the relative amount of emphasis in a particular research design placed on the functional or behavioral significance of the neural analysis. The integrative approach has been used to find relationships between various neural mechanisms and naturally-occuring stimulus-determined behaviors (cf. Ingle, 1976). For example, the dependence of saccade frequency upon the velocity of OKN-eliciting stimuli was reduced or eliminated following lesions in

(1) the area medial to the nucleus of the basal optic root (i.e., the peri-nBOR region), (2) the anterior dorsal tegmental grey, and (3) the large-celled pretectal nucleus, suggesting that all of these structures are involved in mediating OKN (Montgomery, et al., in preparation). A previous study (Lázár, 1973), had shown that OKN in frogs was affected following lesions of nBOR, which had not been demonstrated in other vetebrates. Disruption of neurons extrinsic to nBOR, (i.e., in the peri-nBOR region, and not the nBOR cells), were found to be crucial for the elimination of OKN (Montgomery, et al., in press). The reductionistic approach, which provides the basis for the present study, has been used to examine the specific structural and physiological details of central visual processing (see Scalia, 1976; and Grüsser and Grüsser-Cornehls, 1976 for review), which can further clarify the results of the integrative approach. For example, it was necessary to determine the specific anatomical connections of the nBOR region in order to determine the actual pathways necessary for the mediation of OKN in the frog.

The major visual pathways in anurans have been examined through the visualization of degenerating fibers or terminals following disruption of the optic pathway (Herrick, 1925; Knapp, et. al., 1965; Scalia, et. al., 1968; Lázár and Székely, 1969; Lázár, 1971; and Scalia and Fite, 1974), from the transport of autoradiographic material (Goldberg and Kotani, 1967; Scalia, 1973; Currie and Cowan, 1974; Neary, 1976; Lázár, 1978; Levine, 1978; and Steedman, et. al., 1979), or by anterograde transport of horseradish peroxidase (HRP)

(Scalia and Coleman, 1974; Montgomery, et. al., 1981). The frog possesses (1) major contralateral visual pathways to the pretectum and the optic tectum, with smaller ipsilateral projections to both structures (2) bilateral thalamic projections, as well as (3) an accessory optic system which is predominantly contralateral (see Scalia, 1976; and Montgomery, et. al., 1981). A schematic drawing (Figure 1) of a lateral view of the meso-diencephalic region of Rana pipiens shows the thalamic and tegmental areas as well as the tectal region associated with the retinal projections (from Scalia, 1976). Coronal sections taken throughout the thalamus (Figure 2) can be seen to contain regions which receive bilateral input from retinal ganglion cells, namely, the uncinate neuropil, the neuropil of Bellonci, and the corpus geniculatum. The uncinate neuropil is located between the dorsal segments of the large-celled pretectal nucleus (pp) and the posterior thalamic nucleus (P) shown in Figure 2. The large-celled pretectal nucleus primarily receives contralateral input from the retina (Scalia and Fite, 1974; Wilczynski and Northcutt, 1977), although the specific retinal locus and types of ganglion cells giving rise to this projection have not yet been determined. Also, the entopeduncular nucleus has recently been shown to receive contralateral retinal input. This input previously had been indistinguishable from the corpus geniculatum (Lázár, 1978; Levine, 1980). The thalamic nuclei or cell groups which send their dendrites into either the neuropil of Bellonci or the corpus geniculatum include the lateral geniculate nucleus, the nucleus rotundus, and the

posterocentral and ventrolateral areas. The posterolateral nucleus sends its dendrites into the adjacent posterior thalamic neuropil (Scalia and Gregory, 1970) (see Figure 2). Based on experimental evidence obtained in the present investigation, the posterior thalamic region has been given nomenclature which differs slightly from that used by Scalia (1976).

In addition to receiving projections from the retina, several thalamic areas contain efferents from and afferents to the optic tectum. A large group of bilaterally ascending tectal efferents travel below the lateral marginal optic tract to the lateral neuropil and corpus geniculatum, and contralateral fibers travel to the central gray and ventral pretectal region (Rubinson, 1968). A small group of fibers from the tectum course below the medial marginal optic tract to the ipsilateral pretectum and thalamus (Rubinson, 1968). Contralateral tectal afferents originate from the large-celled pretectal nucleus, the posterior thalamus, and torus semicularis (Wilczynski and Northcutt, 1977). Ipsilateral afferents were found originating in the anterior thalamus (Trachtenberg and Ingle, 1974).

The optic tectum of non-mammalian vertebrates has traditionally been thought to be a crucial "center" for the most complex visual processing. For example, if the optic tectum of the frog is ablated, normal orientation and prey-catching behavior is disrupted (Ingle, 1973b). However, when the tectum is left intact, and the pretectum ablated, normal prey-catching behavior is also disrupted, (Ewert, 1970). Also, although the major retinotectal pathway in the frog

does appear to be necessary for prey-catching and predator avoidance, the presence of this pathway does not appear to be necessary for the generation of either phototaxic or OKN behavior in frogs (Ingle, 1977) or turtles (Hertzler, 1972). These results imply that the retinotectal projection is not the only pathway mediating visually-guided behaviors in anurans, even though the optic tectum has received the most attention in studies of the amphibian visual system, due in part to the complexity of responses and to the accessibility of the region to electrophysiological techniques.

One of the non-tectal visual projection sites, the pretectal nuclear complex, has received some attention with regard to various components of visually-guided behavior, including wavelength discrimination (Kicliter, 1973), OKN (Cochran, et al., 1980), and prey catching in toads (Ewert, et al., 1974) and salamanders (Finkenstadt, 1980). The pretectum consists of both fibers and cell bodies associated with the posterior portion of the posterior thalamic neuropil, uncinate neuropil and the large-celled pretectal nucleus (see Figure 2), which receives input from the retina (Scalia, 1976), and from the optic tectum (Ingle, 1981). In the toad, a knife cut between the pretectum and the optic tectum resulted in disinhibition of tectal cells (Ingle, 1973a; Ewert and von Wietersheim, 1974a, 1974b), and also a disinhibition of prey-catching behavior such that any moving object evoked a prey-catching response (Ewert et al., 1974). However, extracellular recording from areas other than the optic tectum in the frog has been found to be problematical, due to

the difficulty of isolating visual units and the limited time during which a unit can be recorded. Thus, quantitative information on individual units is often difficult to obtain (eg., Fite, et al., 1977). A few studies have reported anuran pretectal units responsive to either a sudden dimming of the entire visual field (von Wietersheim and Ewert, 1978), or to a direction-specificity of movement of large-field stimuli (Cochran, et al., 1980; Katte and Hoffmann, 1980). In addition, caudal thalamic units were reported having large receptive fields (greater than 60°) (Brown and Marks, 1977), and spontaneous activity (Katte and Hoffmann, 1980). However, none of these studies have presented any detailed histological analysis of identified recording sites. It is clearly necessary to differentiate response loci in the pretectal region, since in the insertion of a recording electrode, movement over 100 microns in any direction may result in recordings from either of two visual neuropils.

The pretectum has recently been studied in considerable anatomical detail in several other vertebrates, including fish (Reperant, et al., 1979; Ebbesson and Meyer, 1980; Grover and Sharma, 1981), rat (Legg, 1977; Scalia and Arango, 1979; Robertson, et al., 1980;), rabbit (Collewijn, 1975; Mackawa and Kimura, 1981), cat (Bon, et al., 1977; Itoh, 1977; Abols and Basbaum, 1979; Schoppmann and Hoffmann, 1979; Grahm and Berman, 1981; Hoffmann and Schoppmann, 1981), monkey (Benevento, et al., 1977; Weber and Hutchins, 1982), and tree shrew (Weber and Harting, 1980). The pretectal complex of mammals has been sub-divided into from three to seven distinct cell

masses (Kanaseki and Sprague, 1974; Schoppmann and Hoffmann, 1979), two of which receive bilateral retinal input--the nucleus of the optic tract and olivary nucleus (Berman, 1977). One of these nuclei, the nucleus of the optic tract (NOT), has been implicated in the mediation of OKN, on the basis of the direction-selectivity of extracellularly recorded units and from the observation that electrical stimulation of NOT results in pursuit movements similar to OKN (Collewijn, 1975, 1977; Dubois and Collewijn, 1979). Since units have been found in the frog pretectal region which are also direction-selective, i.e., units which increase their response to movement of a stimulus in the direction which optimally produces OKN, it has been suggested that the frog pretectum is homologous to the mammalian NOT (Cochran, et al., 1980; Katte and Hoffmann, 1980).

The establishment of a homology between the frog pretectum and the mammalian NOT would not only provide further evidence for using the frog central visual system as a model for visual processing, in general, but would also support the continued examination of subcortical brain areas receiving retinal projections. The mesodiencephalic region, which has been shown to be important in the mediation of visually-guided behaviors, is important to an analysis of visual information processing which is closely associated with the output of a visuomotor system. In order to establish homology, however, it is first necessary to determine the precise anatomical details of the afferent and efferent connections of the specific region under study (Hall and Ebner, 1970). Such details have not

been previously worked out for the frog pretectal region. Earlier studies have confirmed that the general pretectal area receives both visual input (cf., Székely, 1971; Scalia and Fite, 1974) and input from the optic tectum (cf., Rubinson, 1968), but the methods used did not permit a detailed analysis of the retinal terminal area or its connections with other CNS regions. The large-celled pretectal nucleus had been previously described as a region of 'loosely arranged large cells' (Székely, 1971), or as the 'large-celled, pretectal nucleus' (Scalia and Gregory, 1970). After soaking a transected optic nerve with HRP in Rana pipiens, the large-celled pretectal nucleus was found to contain a densely labeled center or "core" surrounded by a more lightly labeled region (Montgomery, 1981).

A primary objective of the present investigation was to further increase our understanding of the structural and functional mechanisms underlying visual processing in the leopard frog, Rana pipiens. First, the specific extrinsic connections of the pretectum were determined through the placement of small, localized injections of HRP, specifically in the large-celled pretectal nucleus; secondly, the retinal locus and type(s) of ganglion cells which give rise to this projection were determined. In addition to the anatomical analysis, some response properties of units in the pretectum were determined through the examination of extracellular recordings together with the verification of the specific recording sites. Characteristics of the response properties of units originating from different neuropil regions and nuclei were observed. Specific

attention was paid to the sensitivity of units responding to stimuli which have been used to produce OKN in the frog (Montgomery, et. al., in press). In this way, significant new information bearing upon homology between the pretectum of the frog and the NOT in mammals was obtained.

CHAPTER II

NEUROANATOMICAL ANALYSIS

The Anuran Pretectal Region

Anatomical description of the pretectum of anurans has a long and somewhat confusing history, since similar terms have been used for one of the neuropils associated with primary optic fibers (first observed in the diencephalon), and later for a smaller, more specific region in the anterior mesencephalon receiving a high density of retinal afferents. Historically, areas associated with optic fibers in the diencephalon were divided into two groups, an anterior thalamic group, termed by Herrick (1925), 'the nucleus of Bellonci', and a caudal thalamic group, 'the posterior thalamic nucleus' (Bellonci, 1888). The posterior thalamic region was later differentiated by Herrick (1925), into two groups, a dorso-medial 'area pretectalis,' and a lateral group which he suggested was homologous to the dorsal lateral geniculate nucleus. Both of these areas were supplied by fibers from the marginal optic tract (Herrick, 1925). The lateral group probably corresponded to the posterior thalamic nucleus first described by Bellonci (1888). Much more recently, using Nauta stains, Knapp, et al., (1965), observed retinal axonal degeneration in the presumed 'area pretectalis', and described a series of 'merging' cell groups which were not well-differentiated, except for a group of large 'triangular and fusiform' cells extending obliquely across the

base of the anterior tectal border. This latter group of cells was later described as a 'loosely arranged group of large cells', and was termed the 'nucleus pretectalis' (Lázár and Székely, 1969; Székely, 1971). Thus, what had initially been referred to as a region encompassing both the posterior thalamic nucleus and pretectum, the 'area pretectalis', was now being labeled the nucleus pretectalis to denote a specific, large-celled region situated between the posterior thalamic nucleus and the optic tectum. This group of cells was also termed the 'large-celled, pretectal nucleus' (Scalia and Gregory, 1970), and became known as the 'so-called large-celled pretectal nucleus' (Scalia and Fite, 1974). However, the 'nucleus pretectalis' was described by Lázár (1969), as a 1300 x 500 μm field having a 'hook-like extension in the dorso-medial region' encompassing a much larger region than the large-celled pretectal nucleus. This 'hook-like' region, just rostral to the large-celled pretectal nucleus, was subsequently shown to contain a separate topographic retinal map, based upon the observation of degeneration of optic terminals (Fink-Heimer stain) after localized retinal lesions, and was termed the 'uncinate neuropil' by Scalia and Fite (1974). The present account recognizes this later nomenclature and concentrates upon the anterior mesencephalic region receiving retinal input, the pretectal region, including both the large-celled pretectal nucleus and the uncinate neuropil.

In addition to retinal input, the pretectum receives input from the optic tectum, through a caudal tecto-thalamic tract which

parallels the medial marginal optic tract (Rubinson, 1968). Also, after injection of HRP into the nucleus of the basal optic root, the large-celled pretectal nucleus was found to contain HRP label, suggesting input from the accessory optic system (Montgomery, 1981). The same study showed labeled cells in the large-celled pretectal nucleus following HRP injection into the brainstem. It is clear that there is an incomplete understanding of the complexity of interconnections between the pretectum, specifically the large-celled nucleus, and other regions in the brain. The present investigation took advantage of both the retrograde and anterograde transport capabilities of HRP, and by restricting injections of HRP into the large-celled nucleus, determined the extent of both afferent and efferent connections of this nucleus, as well as clarifying the intrinsic organization of the pretectal region. On the basis of the present findings, changes in some of the nomenclature used to identify several nuclei in the meso-diencephalic region were suggested.

Neuroanatomical Methods

Animals and surgical procedure. Healthy Rana pipiens were maintained on a 12-hour light-dark cycle, at 20-24°C. Frogs were chosen from all seasons, and no seasonal differences were observed in either the

anatomical or electrophysiological results. Prior to the surgical procedure, a frog was immersed in an aqueous solution of tricaine methanesulfonate, at a concentration of 1:500 for 20 minutes. The anesthetized frog was placed on a wooden block designed to hold the head securely between two metal rods. The eyes were kept elevated throughout the electrophysiological experiment with a moistened kimwipe soaked in saline inserted into the mouth, and the frog was maintained under anesthesia in both experiments by covering the body with kimwipes soaked in tricaine (1:500). The frontal-parietal area of the skull was exposed by first making longitudinal and lateral skin incisions, and then folding the skin back. While the skin was clamped out of the way, the surrounding muscle and tissue was dissected away in order to insure that the surrounding blood vessels were not disrupted during subsequent surgery. The cranium was then carefully removed using a dental drill, exposing the dura above the junction between the tectum and the posterior thalamus. Immediately prior to injection (or electrode insertion in experiment II), the protective dura was stripped back, without damaging the dorsal cerebral vascular system.

Injection techniques. Two methods were used to inject HRP into the frog meso-diencephalic region. Pressure injections of .05 - .10 µl 30% HRP (Sigma type VI in distilled water) were made through glass micropipettes having a tip diameter from 20-40 µm. A 1 µl

Hamilton syringe attached to a stereotaxic apparatus and microdrive assembly provided controlled pressure for injection of HRP. In order to produce more controlled and smaller injections, crystalline HRP (Sigma type VI) was implanted into the brain by packing HRP into the tips of micropipettes having an inner diameter of approximately 60 µm. The tip opening, from 60 to 100 µm in length, was made by first filling the pipette with paraffin and then immersing 200 µm of the tip into an ether bath for 5 to 10 minutes, following the procedure of Mori, et al., (1981). The pressure method (using aqueous HRP) resulted in a variable injection size from 300-1000 µm diameter, while the crystalline HRP method resulted in a high density HRP injection size from 100 to 200 µm in diameter.

Immediately after surgery, the block holding the frog was placed into a stereotaxic apparatus modified for frogs. In the frog, stereotaxic coordinates cannot be used reliably, since there is variation in the relative size of the brain and head even for different animals of the same body size and species. Instead, a reference point based on the dorsal surface features of the brain was used to guide the placement of the micropipette. Lesions were made in various thalamic areas in 10 frogs in order to determine coordinates for subsequent penetrations of the large-celled pretectal nucleus. The junction between the two tectal lobes at the midline and the dorsal thalamic surface was used as a reference for the stereotaxic apparatus. Thus, at least for the pretectal region, each initial penetration was within ±200 µm of the desired locus.

Histological procedure. The injections were followed by post-operative survival of 3 to 5 days. The frog was anesthetized in tricaine methanesulfonate (concentration 1:500) for 25 to 30 minutes and then perfused transcardially with 30cc of saline followed by 80cc of 1.25% gluteraldehyde and 1% paraformaldehyde fixative in a 0.1M phosphate buffer (pH 7.2). The brain was excised and placed in fixative for 2-3 hours, followed by immersion in 30% sucrose-buffer overnight at 0-4°C. The brain was then embedded in 20% gelatin, frozen, serially sectioned from 40 to 50 µm and reacted according to a modified Hanker-Yates (Hanker, et al., 1977) protocol for demonstrating HRP reaction product (See Montgomery, et al., 1981). Sections were counterstained with cresyl violet and examined under a light microscope for HRP label. Immediately following perfusion, the eyes were removed, the cornea, lens and vitreous excised, and the whole eyecup placed in fixative for 2 hours. The eyecup was then washed in several changes of phosphate buffer (pH 7.2), reacted at 0-4°C in Hanker-Yates reagent for 2 hours, washed in phosphate buffer again, and imbedded in 20% gelatin. In addition, several eyecups were reacted in a Hanker-Yates protocol for staining wholemount retinas (Stone, 1981). This process uses cobalt chloride as an enhancement for HRP reaction product, together with incubation in double strength Hanker-Yates Reagent. Horizontal, transverse serial sections were cut from top to bottom of the frozen eyecup. Sections 20 µm thick were sampled every 100 µm, and the serial sections around any section containing HRP label were subsequently mounted and

examined under a light microscope. Sizes of cells in both the pretectal neuropil and the retina were classified on the basis of the size and shape of their somata.

Neuroanatomical Results

General features of the pretectal region. A schematic representation of cell groups throughout the frog brain is presented in Figures 3-8. The terminology used in the following presentation differs from that of Scalia (1976), based on both the present findings and other recent investigations (cf. Wilczynski and Northcutt, 1977). The caudal portion of the posterior thalamic nuclear group (terminology of Neary, 1975), can be divided into dorsal and ventral components on the basis of morphology and connectivity, following HRP injections confined to the large-celled pretectal nucleus (cf. Figures 9A and 9B, case #21). This posterior thalamic group (Pd and Pv) corresponds to the previously labeled central grey region (Scalia, 1976, Figure 2). The dorsal posterior thalamic group (Pd) contains cells with restricted dendritic fields related to the posterior commissure and the uncinate neuropil (U), whereas the ventral posterior thalamic group (Pv), has extensive dendritic fields reaching the large-celled pretectal nucleus (LcPt) (Figure 5, bottom). Cells in Pd bilaterally project to laminae 8 and 9 of the optic tectum (terminology of

Székely and Lázár, 1976), while cells in Pv project to the ventral brainstem, near the abducens nucleus (nVI) and the nucleus reticularis medius (NRM). This terminology differs from that of Montgomery, et al. (1981), which also described the posterior thalamic groups as regions of central gray. Superior to Pd and Pv and lateral to the posterior commissure (dotted line in Figure 5), is a migrated cell group, the postero-dorsal division of the lateral thalamic nucleus (Lpd). This corresponds to the dorsal portion of the posterolateral nucleus of Scalia (1976), shown in Figure 2. Caudal to this region is the nucleus of the posterior commissure (nPC) and a region of pretectal gray (PtG), lying medial to nPC, both of which project to LcPt (Figure 6, top, not shown in Figure 2).

Afferents to LcPt. In the present study, the contralateral retina was examined for the presence of HRP-labeled ganglion cells in cases which showed localized HRP injection into LcPt. Three general size categories of ganglion cells were found to be HRP-positive in these cases, including a large, 20-30 µm diameter cell, medium, 10-20µm, and a small, 7-10 µm diameter cell (Figures 10-12). The dendritic arborizations in specific retinal layers could not be determined. A total of 71 ganglion cells were counted in one case (#33) which showed injection specific to LcPt (Figure 13). The common feature of the retinal projections to LcPt for both case #33 and for a larger injection involving LcPt (Montgomery, et al., 1981), was the

restriction of cells to the central area of the retina (Figure 14). This pattern of distribution is similar to the distribution of highest ganglion cell density in the eye of Rana pipiens (Carey, 1975) (Figure 16). The labeled retinal region corresponds to approximately a 40° x 30° elliptical region of visual space extending obliquely across the visual field of one eye (Figure 15). Assuming the ganglion cell lies at the center of its receptive field, then the field of view corresponding to the region of labeled ganglion cells can be expanded by 8°, since the largest excitatory receptive fields of retinal ganglion cells observed in Rana esculenta retina are about 15° for class 4 neurons (Grüsser and Grüsser-Cornehls, 1976). This expanded region is represented by the dotted line in Figure 16.

The course of optic afferents to LcPt has been previously identified in cases showing anterograde transport of HRP following optic nerve soak (Montgomery, et al., 1981, Figure 17). Input is mostly contralateral from the axial optic tract and the lateral marginal optic tract; however, a smaller ipsilateral component is also present. Brains cut both in the coronal and and saggital planes identified the elliptical extent of the retinal projection, roughly 700 x 350 µm in the coronal plane, extending 550 µm in the saggital plane. The projections from the retina terminate into a dense-core (240 x 120 µm diameter) region in the center of LcPt, containing a few large cells along the margins of the dense-core (Figure 18). It has been suggested (Montgomery, personal communication) that this margin is the region through which the axial

optic tract fibers enter LcPt. The dense-core region is surrounded by a more loosely packed smaller cell region and can be observed through anterograde transport of HRP following an injection into the pretectal gray (PtG) (Montgomery, et al., 1981, Figures 19-21).

In addition to retinal input, the LcPt was shown to receive afferents from (1) the ipsilateral optic tectum, (2) the nucleus of the basal optic root (nBOR), (3) the anterior thalamus, and (4) the nucleus of the posterior commissure (nPC), following HRP injections confined to LcPt (cf. Case #21, Figures 3 through 9), or the optic tectum (Montgomery, et al., 1981). The tectal projection originates from the ascending tectal bundle located medial to the lateral marginal optic tract, through fibers originating from layers 8 and 9 of the lateral tectal lobe (case #17). Both anterograde and retrograde transport of HRP have been used to demonstrate afferent projections from nBOR to LcPt. HRP injections into LcPt resulted in retrograde labeling of ganglionic neurons within nBOR (case #4, Figure 22), while injections of HRP into nBOR (Montgomery, et al., 1981), resulted in the anterograde labeling of an axonal bundle arborizing in the dense-core region of LcPt. Following injections restricted to LcPt, cells were labeled via retrograde transport of HRP in the anterior thalamus, in the nucleus rotundus (case #21, Figures 4 and 23), as well as in nPC.

Neural organization of the pretectal region. Within the retinal

terminal field of LcPt, three types of neurons were observed; large, elongated cells, 25 µm in diameter; medium elongated cells, 12-13 µm diameter; and small stellate cells, 7.5 - 9 µm in diameter (Figure 18). Results from previous intraocular proline injections (Montgomery, et al., 1981) and HRP injections into the mesencephalic torus and PtG regions indicate that the dense core region of the nucleus is relatively cell-free (Figures 20 and 21), containing only a few small neurons. The large neurons can be seen to cluster along the margins of the dense-core region. The large cells have both long apical dendrites 200 µm in length, which typically extend along the ventrolateral axis of the nucleus, and two basilar dendrites emerging from the soma, one of which extends into the opposite direction from the direction of the apical dendrite (Figure 18). The stellate neurons have 2 or 3 dendrites within a 90µm diameter field, and appear to be intrinsic to LcPt.

Two other extrinsic neuronal populations send their dendrites into LcPt. The group most proximal to LcPt is located dorsal to the posterior commissure and intermediate between LcPt and the tegmental gray, and has been termed the 'pretectal gray' (PtG) (Figures 6 and 24, 25). The more ventral segment of PtG is postsynaptic to LcPt, whereas the dorsal segment is postsynaptic to the uncinate retinal terminal field. There are two basic types of cells in the region of PtG postsynaptic to LcPt, spindle-shaped neurons 12 µm in diameter, having apical dendrites in LcPt, and candelabra-shaped neurons 15 µm in diameter, having two apical dendrites branching within LcPt.

The second group of extrinsic neurons is located in the most superficial layers of the posterior thalamic nucleus medial to LcPt (Figures 26-28). Two basic cell types were found postsynaptic to LcPt in Pv (case #18); large, pear-shaped neurons 12-17 µm in diameter having 2 to 3 short basilar dendrites extending into Lpd, and long (480 µm) apical dendrites branching within LcPt (Figures 27 and 28). Smaller spindle-shaped neurons, 10 µm in diameter, having short apical dendrites branching close to their somas, comprise the other cell group. HRP injections into the Pv region resulted in retrograde label in neurons located in the caudal portion of the nucleus of the medial longitudinal fasciculus (nMLF, Figure 6), near nIV (case #19).

Efferents of LcPt. Two distinct projection systems appear to originate from the LcPt. The first arises from the ventral LcPt and courses ipsilaterally and dorsally through the marginal optic tract region to the most superficial layers, 7, 8 and 9, of the optic tectum (Figure 5). These fibers terminate in the anterior and caudolateral portion of the tectal lobe, and not in the caudo-medial portion of the tectum (cases #18, 21, 33). A second projection system courses ventrally from the LcPt along the lateral margin of the tectum through the region of the torus through the nucleus reticularis tegmenti (nRT), where terminal endings can be observed (Figure 7). A small number of fibers also descend directly to the

dorsal margin of nBOR. HRP injections of nBOR resulted in labeling of fibers in the dense-core region of LcPt, thus demonstrating reciprocal connections between these two nuclei (Montgomery, et al., 1981). This projection system terminates in a region medial to the superior olive nucleus (SO), near the abducens, nVI (Figure 8).

CHAPTER III

ELECTROPHYSIOLOGICAL ANALYSIS

Recording from the Pretectal Region

The anatomical analysis of the pretectal region of the leopard frog shows a complexity of interconnections previously unrecognized. Extracellular recordings from single units in the pretectal region can be used to determine possible functional correlates of these complex interconnections. There have been relatively few studies which have examined the response properties of single units from caudal thalamic regions in the anuran brain (Ewert, 1971; Vesselkin, et al., 1971; Brown and Ingle, 1973; Brown and Marks, 1977; Gaillard and Galand, 1979; Cochran, et al., 1980; and Katte and Hoffmann, 1980). Also, with one exception (Brown and Marks, 1977), previous studies which provided single-unit analysis from visual areas other than the optic tectum in the frog typically report between 20 and 70 well-isolated units (cf. Gaillard and Galand, 1979), whereas studies of superficial tectal layers characteristically report between 100 and 350 units (cf. Gaze and Keating, 1970). Recording from non-tectal areas has generally led to classification of units into groups of specific response characteristics, i.e., on the basis of differences between units, instead of groups based on general response characteristics, or similarities, among units. Not only is the total number of recorded units relatively small, but also the amount of

time in which a unit can be recorded from is limited. Recording times of under one hour allows only a few measures to be taken, depending on the type of stimulating and recording apparatus being used. These considerations limit in-depth quantitative analysis of response properties, since the determination of general response characteristics requires the presentation of many stimulus trials over an extended period of time, up to three hours. In the present study, responses were obtained from extracellular units recorded in the pretectal region in the leopard frog. Particular emphasis was placed on the response of the units to stimuli which produce horizontal OKN, since OKN has recently appeared to be mediated through the pretectal region in both frogs (cf. Cochran, et al., 1980; Montgomery, et al., 1981), and mammals (cf. Collewijn, 1975). A moving black-and-white striped pattern was projected onto a screen directly in front of the frog's binocular field of view. This stimulus has previously been used to reliably evoke OKN in behavioral studies on the frog (Montgomery, et al., in press).

Previous studies have reported caudal thalamic units in the frog which have (1) relatively large receptive fields (greater than 60°) (Brown and Marks, 1977), (2) the presence of spontaneous activity (Katte and Hoffmann, 1980), and (3) direction selectivity (cf. Cochran, et al., 1980). Such response characteristics might be expected of units that produce or mediate OKN. The present study sought to relate these previous findings to the specific loci giving rise to such unit responses, since previous reports have not

considered the presently recognized number and anatomical complexity of mesodiencephalic visual areas when examining unit responses. Elucidation of response properties of single units in specific visual areas, combined with an examination of the interconnections of those regions could ultimately provide an increased understanding of the visuomotor or oculomotor systems mediating OKN.

Electrophysiological Methods

Animals and surgical procedure. Healthy Rana pipiens, from all seasons, were maintained on a 12-hour light-dark cycle, at 18-24°C. No differences in the response characteristics were measured during different seasons. The same surgical procedure was followed as described in Experiment I, in order to expose the thalamo-tectal junction prior to electrode insertion.

Microelectrode and recording apparatus. The recording and lesioning electrodes were Woods-metal-filled glass micropipettes. Electrodes were pulled with a David Kopf vertical pipette puller (model 700C) to a tip diameter of 2 to 10 microns. The pipettes were filled with heated Woods-metal and plated with gold and platinum, following the procedure of Dowben and Rose (1953). This procedure has been

determined as giving the best signal-to-noise ratio for recording in the frog central nervous system (Lettvin et al., 1959; Fite, 1969). Electrode impedence for electrodes with tip diameters of 5-10 microns measured between .1 to 5 megohm (1000Hz), using a Frederick Haer Impedence Checker.

Unit activity was amplified with a Grass P511 preamplifier, and was recorded on magnetic tape for further analysis during the experimental procedure. Unit responses were also passed through a Frederick Haer signal enhancer module, which was set to produce an optimum signal-to-noise ratio for the units under investigation. Unit activity was displayed on a dual-channel Tetronix model 502 oscilloscope with an audio amplifier and speaker combination in use for listening to unit activity. A Frederick Haer amplitude analyzer was used to analyze single-unit activity, through a movable 'window' which selects a specific range of amplitude from the input and sends out a signal corresponding to all the events which occured in the amplitude range specified. The output of the amplitude analyzer was sent to a Gerbrands digital counter, in order to determine preliminary analysis of the number of spikes during a given stimulus presentation. This also allowed a choice of one set of spikes over another in the multiple-unit recording situations. A Tetronix model 5113 dual-beam storage oscilloscope was used to verify individual unit waveforms and for spike-train analysis.

Stimulating apparatus. A modified film strip projector having a 120 volt, 300 watt bulb, (reciprocal color temperature of 303 mired), was designed to produce a continuously variable moving stimulus which was rear-projected onto a tangent screen and which filled a large portion of the subject's frontal field of view of one eye or 3/4 of the anterior binocular field of view. The luminance of the screen was 16 cd/m^2, as determined by a Tetronix model J16 digital spectrophotometer. The stimuli included shadows, lines, and an OKN striped pattern of the same periodicity used in behavioral OKN studies (Montgomery, et al., in press). The projector was fitted with a dove prism which, when rotated to various positions, allowed movement of the stimulus in any plane across the screen. The range of pattern velocities used was from 10° to 50°/sec, which covers the velocity range over which OKN can be evoked behaviorally.

A large aluminum sphere (40cm radius) having a white inner surface was used to determine receptive field properties and positions of the visual units encountered. Circular black targets of 5, 12 or 32 mm, subtending .72°, 1.7°, or 13.8° of visual angle, respectively, were moved across the inner surface with a hand-held magnet moved on the outer surface. The outer surface of the sphere was calibrated in radial coordinates. At 50cm from the frog, the sphere subtended about 120° of visual angle, covering the major portion of the frontal, binocular field of view when the center was aligned with the axis of the midpoint between the eyes (Fite, 1973). Since, at 50cm, the frog is emmetropic (cf. Grüsser and Grüsser-Cornehls, 1976), this resulted

in conservative estimates of the size of receptive-fields. About 2/3 of the field of view was covered when the center of the sphere was aligned with the optic axis of one eye. A movable tungsten light provided even illumination of the hemisphere, at 38 cd/m^2.

For determining a unit's response to chromatic stimuli, an American Optical Photoilluminator having a 19 volt, 150 watt GE quartzline bulb (592 mired) was used to project via a fiber optic bundle and in Maxwellian view (cf. Carterette and Friedman, 1975), chromatic stimuli produced by Bausch and Lomb narrow-band interference filters having a half-bandwidth of 8-10nm. The peak wavelengths were at 433, 460, 499, 524, 558, 576, 600 or 625nm. The intensity of the chromatic stimuli were controlled with neutral-density filters, and the 600 nm and 650 nm filters were used in conjunction with a short wavelength cutoff filter (Wratten #21). Maximum luminance was 45 cd/m^2. Characteristics of the interference filters and neutral density filters had been previously determined using an ISCO spectral radiometer (Fite, et al., 1977).

Extracellular recording procedure. Frogs were anaesthetized throughout the experiment by covering with kimwipes saturated in tricaine methanesulfonate. The frog had to be maintained at the proper level of anesthesia in order to record from any units. Several times during the investigation of response properties, the anesthesia level decreased such that a disruption of isolated

responses occurred, possibly due to increased respiratory and cardiovascular activity in the brain near the electrode insertion point, resulting in large DC-shifts and noise produced rhythmically. Conversely, a general response decrement was observed in all visual areas, including the optic tectum, when the frog was too deeply anesthetized.

In order to locate units which would respond to visual stimuli, a search pattern was started approximately 1200 μm lateral and 200 μm caudal to the junction between the midline of the tectal lobes and the dorsal thalamic surface. Penetrations continued medially at depths centered around 1000 μm, until a unit was encountered which spiked as a result of stimulation from a hand-held flashlight, and could be adequately isolated from neighboring units, using the amplitude analyzer, if multiple units were present. The initial criterion for identification of a single unit was a relatively uniform size of the action potentials.

Once a unit was isolated, the test for a response to moving OKN stripes and lines preceded all other analysis, due to the variability in the amount of time the electrode could remain near the unit (typically from 5 to 60 minutes). The use of a moving film-strip projector allowed the stimuli to be repeated in the same configuration, i.e., direction and velocity, for several trials. Thus, any variability in the response occuring as a result of adaptation or the inclusion of responses from other units could be ascertained. Responses to several stimulus orientations and

velocities were obtained from most units. Following the OKN stimuli, general receptive field characteristics were ascertained -- the relative size of the field, whether binocular or monocular, if sustained or transient responses could be evoked, and whether or not any habituation occured. For units which were isolated for the longest periods, responses to different wavelengths were determined using a threshold-criterion method (Fite, et al., 1977). A threshold-criterion response was defined as 1-2 spikes occuring on 3 out of 5 repeated stimulus presentations. The chromatic stimuli were presented monocularly in Maxwellian view at .5 sec. duration, every 20 seconds. In addition to visual stimuli, various auditory and tactile stimuli consisting of clicks, claps, and vocalizations from the experimenter, or a light touch from a paintbrush to the nose or limbs, were employed to determine multimodal unit response properties, i.e., responses to either noise or touch in addition to visual stimuli. The basic response measure for these stimuli was either the total number of spikes or the number of spikes per second occuring after a given stimulus presentation.

Verification of recording sites. Immediately after the responses had been obtained, (or were lost after some information had been recorded), a small electrolytic lesion was made by passing a current of 5 μ amps for 5 seconds (electrode positive). No more than 3 neighboring units within 100 μm were recorded in a single electrode

penetration before a lesion was made, thereby ensuring accurate localization of the recording site. After a post-lesion survival of about 24 hours, the frog was again immersed in tricaine methanesulfonate (conc. 1:500) for 25-30 minutes. The frog was then perfused with saline, followed by a modified Clarke's fixative, containing 95% absolute alcohol and 5% glacial acetic acid. The brain was excised, dehydrated with a series of cellosolve followed by cholorform, and then embedded in paraffin. The brain was then sectioned in serial 10 micron segments coronally, on a rotary microtome. Sections were taken through the thalamus up to the level of the anterior tectum. The sections were then stained with a modified Klüver (luxol-fast blue and a neutral-red) stain, which provides an optimal visualization of lesion sites, cell bodies, and fibers.

Electrophysiological Results

General response characteristics. Much of the information obtainable on the response properties of cells in the pretectal region of *Rana pipiens* is qualitative rather than quantitative, since detecting and holding units for any reasonable length of time necessary to gather quantitative information occurred for only about half of the units presented here. Lesions following each recording from LcPt are

presented in Figures 29 and 30. The following summary represents the results of over 250 penetrations on 48 Rana pipiens brains, and a total of 17 well-isolated visually responsive units, 13 of which are from different frogs. All lesion sites are presented schematically in Figure 31. Unless otherwise noted, single units characteristically demonstrated a large negative component to their waveform (Figure 32). The signal-to-noise ratio for most units was rather low, due to the electrode configuration, which had to be kept large (3-10 μm tip diameter) in order to produce stable conditions throughout the series of repeated penetrations. Responses were presumed to be primarily from post-synaptic sites and not from optic fiber input, since the type of responses were not typically characteristic of optic fiber recordings (Grüsser and Grüsser-Cornehls, 1976). Responses from most units were binocular, further indicating that they were postsynaptic. Presumably, responses from the pretectal gray region could not have been from first-order optic terminals, since there is no known direct retinal input in this area.

A wide variety of response types was observed in the pretectal and surrounding regions. In general, every unit responded to the offset of either a small, hand-held flashlight (luminance = 1000 cd/m^2) or to the offset of the general room illumination (room lights on = 30cd/m^2). Response was greater for light offset than onset in 47% (n=8) of the units encountered, with 12% (n=2) having no 'on' response at all, and 12% (n=2) having a greater 'on' response to light stimulation than 'off' response. The remaining units 29% (n=5)

showed equal responses to the onset and offset of light. All of the units showed transient rather than sustained responses to either light onset or offset, (or to changing stimulus features), which typically consisted of a burst of spikes. Only 24% (n=4) of the units encountered maintained spontaneous activity in the dark, unlike previous reports that 95% of the thalamic units could be spontaneously active (Katte and Hoffmann, 1980). This discrepancy could be due to the fact that in the present study spontaneous activity was not used as a criterion for thalamic units, unlike the Katte and Hoffmann (1980), study. Two basic types of unit responses to OKN stimulation were observed: units which spiked following either the onset or offset of stimulation, or both (29%, n=5, 'bursting' or transient units, Figure 33), or units which maintained or decreased an ongoing train of spike activity throughout the presentation of OKN stimulation (29%, n=5, 'sustained' units). Fifty-three percent of the units (n=9) had medium sized receptive fields, 20-40°, while 6% (n=1) had small receptive fields, less than 20° in diameter. Several units could not be held long enough to gather precise receptive field information. These results are summarized in Table II.

Large-celled pretectal nucleus. Two units recorded from the large-celled pretectal nucleus (LcPt) (#13, #14), responded similarly to OKN stimulation. Both units responded to a horizontally or vertically oriented moving striped pattern (vOKN or hOKN,

respectively), but differently than they resonded to either a single moving line having the same stripe width and length as the OKN pattern components, or to a moving shadow. At the slowest speed, 10°/sec, both units responded with spikes throughout the duration of the moving OKN stimulus presentation, in all orientations and directions. Stimulus velocities greater than 15°/sec resulted in only onset and offset responses, with bursts of 8 spikes/sec to the onset and 3 spikes/sec to the offset, with no sustained spiking throughout the stimulus presentation. No directional selectivity was observed; however, response to oblique OKN stimulus orientations was reduced to about 2/3 of the response to either hOKN or vOKN, suggesting that these units were differentially responsive to the orientation of the OKN stimulus. Response to movement of oblique single lines was the same as response to a horizontal or vertical moving line, although the response was approximately 30% greater to smaller line thicknesses (4° vs 8°). These LcPt units also responded differentially to chromatic stimuli, with a lower threshold 'on' response occurring to wavelengths between 524 and 576nm than to wavelengths above 576 nm or below 524 nm.

Pretectal gray. A total of 7 units were recorded from the pretectal gray region (PtG), three of which showed spontaneous activity in addition to transient responses to changes in stimulation (see Table II). The units showing no spontaneous activity in this region had

stronger responses, (measured as increases in spike rate), to stimulus offset than to stimulus onset, while 3 spontaneously active units had either equal transient response to light onset and offset, or a greater transient response for light onset. However, the characteristic spontaneous activity occurring in the dark (from 1 to 5 spikes/sec) decreased to 25% of that activity when a light was turned on (Figure 33), an effect which lasted for approximately 10 seconds. The percent of activity of the unit was defined as the average number of spikes per second occurring during three different stimulus presentations, each of which lasted an average of 5-10 seconds, times 100.

One of the spontaneously active units (#18) demonstrated a gradual decrease in firing rate for decreasing OKN stimulus velocities below 50°/sec, measured at the slowest velocities (ca. 10°/sec). The other spontaneous units decreased their rate of spontaneous activity to about 50% of the rate in the presence of a stationary OKN stimulus, for stimulus velocities around 25°/sec (Figure 34), and showed no change in firing rate for stimulus velocities above or below 25°/sec. Spontaneously active units either responsed to a wide range of OKN stimulus velocities, or were 'tuned' to a fairly narrow (±5°/sec) range of OKN stimulus velocities. These units showed a decreased response (15%) for vOKN which typically produced the maximum decrease in spike rate for the two narrowly-tuned units. Either direction for vOKN, (dorsal-ventral or ventral-dorsal movement), resulted in the same response decrement in

spontaneous spike rate. For hOKN, there was a slight decrease in spike rate (15%) to stimulus movement in the temporal-nasal direction compared with movement in the nasal-temporal direction.

Two other PtG units characteristically showed a transient response to the onset and offset of OKN stimulation. The response of one unit consisted of bursts of 4-5 spikes when a change in velocity greater than 2.5°/sec occurred, for either vOKN or hOKN in any direction, thus 'acceleration' or velocity change was important for this unit's responsiveness, while the other units showed no such sensitivity. It should be noted that a large-field shadow moving in any direction produced a burst of 10-12 spikes/sec, for both units, and that the response to a single line of any orientation moving through the receptive field consisted of a single spike burst of 5 spikes/sec.

Posterodorsal division of the lateral thalamic nucleus. Three units recorded from the posterodorsal division of the lateral thalamic nucleus showed very complex response properties. One unit (#15) produced an average burst of 16 spikes/sec in response to the offset of general illumination, and a short burst of 3 spikes to the onset of illumination. A large-field shadow moving in either the ventral-dorsal direction or nasal-temporal direction produced a burst of 22 spikes, whereas movement in either the dorsal-ventral or the temporal-nasal direction produced only half of the response (10

spikes). This unit's response resembles the response characteristics of class-3 ganglion cells, which can have directional-selectivity (Grüsser and Grüsser-Cornehls, 1976). Response of this unit to hOKN stimuli in either the nasal-temporal or the temporal-nasal directions at 10°/sec resulted in 10-12 spikes at a rate of 5 spikes/sec following the onset of OKN stimulus movement. Increasing the velocity of stimulus movement to 20°/sec increased both the number of spikes (to 15-20) and the average spike rate (to 7.5/sec). Velocities greater than 20°/sec subsequently resulted in a continuous decrease in the number of spikes per burst and the spike rate. In addition, the termination of OKN stimulus movement in the nasal-temporal or dorsal-ventral directions for velocities less than 15°/sec resulted in a delayed after-discharge of 14 spikes at the average rate of 4.7 spikes/sec, which occured one second following the cessation of pattern movement. Movement of the OKN stimulus in either the temporal-nasal or ventral- dorsal directions produced no delayed afterdischarge. Also, response to oblique OKN in any direction consisted of a burst of 6 spikes at 3 spikes/sec following the onset of stimulus movement at any velocity up to 50°/sec, and resulted in no burst or after-discharge to the offset of the OKN stimulus.

The other two units (#16a, #16b, Figure 35), encountered in Lpd did not respond to movement of the OKN stimulus in any direction. One unit (#16a) did respond to a vertical white line moving in any direction with a burst of 2-3 spikes, but did not respond to movement of a horizontal white line in any direction. The other unit (#16b),

showed response to a moving shadow in either the nasal-temporal or the temporal-nasal direction with a burst of 20 spikes at 20 spikes/sec, but showed no response to movement in the dorsal-ventral or ventral-dorsal directions. This unit had to be light adapted for at least 30 seconds before responding to the offset of general room illumination, with 18 spikes at 10 spikes/sec.

Anterior margin of the ventromedial optic tectum. Three units were recorded in regions lying between the ventromedial optic tectum and the posterolateral portion of the thalamus. The response of these units resemble class-4 ganglion cells (Grüsser and Grüsser-Cornehls, 1976). All units were either exclusively or primarily responsive to light offset, with 14-20 spikes at 5-10 spikes/sec. All units showed a response to a rapidly moving shadow at speeds greater than 25°/sec with bursts of 8-10 spikes at 6 spikes/sec. In addition, one unit (#1) showed a 1 spike/sec discharge in the presence of slowly (10°/sec) moving hOKN stimuli in either direction, temporal-nasal or nasal-temporal. No measurements could be obtained for vOKN movement. One unit (#12) increased its rate of firing from 1 to 3 spikes/sec for movements of either a horizontal or vertical line through its receptive field. This unit showed no differential responses to chromatic stimuli when measuring the rate of spikes/sec as opposed to the total number of spikes.

Dorsal posterior thalamic nucleus. One unit was recorded from the dorsal region of the posterior thalamic nucleus (Pd). This unit was an 'off' unit, responding to either the offset of the general room illumination or to a hand-held flashlight with a burst of 5-8 spikes. However, the 'off' response would only occur if the interval between onset and offset of the light were sufficiently small, less than 1 sec. Otherwise, no spikes would occur.

Multimodal units. Approximately 15 units which responded to both tactile as well as visual stimuli were encountered in both the pretectal gray region and the dorsal posterior thalamic nucleus. Auditory units were also encountered in deep penetrations (below 1200μm) through the pretectal gray region.

CHAPTER IV

DISCUSSION

Neurobiological Analysis of the Pretectal Region

Relevance of the present study to the discipline of psychology. Psychology is often described as a diverse science, one which uses information and techniques from several disciplines, including biology, chemistry, physics, mathematics and neuroscience. Although the present study is a neuroscientific analysis, it does have relevance to the understanding of behavior, since the neural mechanisms under investigation appear to be involved in several stimulus-determined behaviors. An identification of the physiological mechanisms in the frog brain underlying visually-guided behaviors should begin with a thorough and detailed anatomical description. The 'link' between neural mechanisms and behavior has often been demonstrated by ablation studies. With respect to the present investigation, it has been previously shown that the removal of either the large-celled pretectal nucleus or the posterior thalamic nucleus resulted in a decrease in the frequency of saccades during OKN stimulation (Montgomery, et al., in press). Thus, these pretectal regions were shown to be directly or indirectly involved in the mediation of OKN. In addition to OKN, the pretectum of anurans has also been implicated in prey-catching and predator avoidance behaviors (cf. Ewert and von Wietersheim, 1974a, 1974b). For example, a knife-

catching responses to irrelevent stimuli. Also, the caudal thalamic and pretectal regions appear to be involved in stationary object detection, since frogs with fairly large caudal thalamic lesions were unable to avoid stationary barriers (Ingle, 1981).

The present study has clarified both the anatomical extent of specific pretectal cell groups and the afferent and efferent connections of the large-celled pretectal nucleus (LcPt). These results can be used as a basis for further investigations which are concerned with understanding the functional or behavioral significance of certain neural cell groups and pathways in the frog pretectal region. Responses were recorded from several pretectal areas and were compared to the general response characteristics previously recorded in the caudal thalamic-pretectal region. Specific attention was paid to unit responses to OKN stimuli, since the behavioral response to OKN stimulation is elicited by specifiable stimulus configurations. Electrophysiological responses may be used to assess functional correlates of anatomically defined regions implicated in the mediation of OKN. Specification of the neural correlates of OKN is facilitated since there is little modification of the behavioral response to OKN stimulation by learning or experience. The present study can, therefore, be considered as psychologically relevant, through the investigation of anatomical and physiological correlates of OKN, particularly in relation to recent behavioral-ablation experiments.

The pretectum of frogs and mammals: A possible homology? In the present study, a homology between LcPt in frogs and NOT in mammals was strongly supported by the anatomical findings and to a lesser degree by the electrophysiological results. In the pretectal complex of the cat, intraocular injections of tritiated amino acids resulted in the labeling of two cell groups, the olivary pretectal nucleus and the nucleus of the optic tract (NOT) (Berman 1977). Previous studies had described the posterior pretectal nucleus of the cat as receiving direct projections from the retina; however, Berman (1977), determined that the retinal terminals were just outside the posterior nucleus. The pretectal complex of mammals is thought to be involved with a variety of visually-guided behaviors (cf. Berruluchi, et al., 1972; and Collewijn, 1977), the pupillary light reflex (cf. Carpenter and Pierson, 1973), and visual attention (Winterkorn and Meikle, 1981).

In the frog, two pretectal groups, the uncinate neuropil and the large-celled nucleus (LcPt), both receive first-order retinal projections (cf. Scalia and Fite, 1974). The pretectal region of anurans has been implicated in the production of behaviors analogous to those found in the mamalian species, such as OKN and pattern detection, and in the mediation of visually-guided behaviors such as prey-catching and predator avoidance. Thus, an increasing body of evidence supports the possible homology of the anuran LcPt and mammalian NOT (see also Mayr, 1970; Hodos, 1970).

Retinal projections to LcPt. The present study of the frog pretectal region has clarified several neuroanatomical relationships, both afferent and efferent. The primary afferent projection originates from retinal ganglion cells located in the central retina (Fig. 14), from a region which corresponds to the area of highest ganglion cell density in Rana pipiens (Carey, 1975). The corresponding representation in visual space of this region containing HRP-labeled ganglion cells extends into an elliptical 60° x 100° region (Fig. 16) (Gaillard and Galand, 1979). This places the combined projections from both eyes within 20° of the midline. Thus, the region of visual space corresponding to the representation of LcPt can be seen as a fairly wide (60°) band extending approx. 220° around the center of the visual field (the midline between the two eyes). The shape of this visual representation is consistent with possible mediation of OKN, since large-field stimuli traveling along a perimeter about the horizontal meridian do elicit OKN. The projection of the cat retina to the nucleus of the optic tract (NOT) also originates primarily from a horizontal band which includes the area centralis (Ballas, et al., 1981), suggesting further evidence for homology between the NOT and the anuran LcPt based on the distribution of the retinal projections. The largest HRP-labeled ganglion cells following LcPt injections were found in the periphery of the centrally labeled region (Fig. 14), also similar to the projection from retina to NOT in the cat (Ballas, et al., 1981). In the cat (Ballas, et al., 1981), few large ganglion cells were found projecting to NOT and

similar results were observed in the present study.

In the present study, approx. 71 large, medium and small ganglion cells were retrogradely labeled with HRP following apparently complete and exclusive injection of LcPt. This follows a similar pattern of retinal labeling following an injection which included both LcPt and deep tectal layers (Montgomery, et al., 1981). This indicates that either there was minimal, if any, tectal involvement in the latter injection, or the tectal projection comes from similar retinal regions. Figure 14 shows the numbers of the three types of ganglion cells projecting to LcPt, with the large cells comprising only 4% of the total labeled cells.

Two neuronal populations extrinsic to LcPt. Two regions located outside LcPt have dendrites which extend into the terminal field of LcPt and should, therefore, be considered as part of the pretectal efferent system. One of these regions, the posterior thalamic nucleus, (terminology of Neary, 1975), was subdivided on the basis of morphology and connectivity of its elements. The dorsal portion (Pd) has cells which send dendrites into the nucleus of the posterior commissure (nPC), and into the uncinate neuropil (U). The ventral posterior thalamic group (Pv) contains the specific population extrinsic to LcPt, which contains dendrites from cells in the four most superficial laminae of the posterior thalamic nucleus (see Fig. 26A). Interconnecting fibers between Pd, Pv and other areas appear

at the ventral region of this area. In addition to the pretectal connections, cells in Pv bilaterally project to laminae 8 and 9 of the optic tectum. Injection of HRP into Pv (case #19), resulted in HRP label in the region of nVI, and in the nucleus reticularis medius. The other extrinsic nuclear group, the pretectal gray (PtG), sends its dendrites into LcPt (Fig. 24A). The interconnections of this region with other brain regions have not yet been determined. Unit responses in the present study indicate that the PtG region may be an important locus in the mediation of OKN.

Afferents to and efferents of LcPt. The large-celled pretectal nucleus has been shown to receive afferents from ganglionic neurons in the nucleus of the basal optic root (nBOR), which is a first-order retinal projection site (Fig 22A, Montomgery, et al., 1981). The LcPt also projects to the margins of nBOR, suggesting the existence of reciprocal connections with the accessory optic system (AOS). In addition to the projection to LcPt, the peri-nBOR region sends fibers through the nucleus of the medial longitudinal fasciculus (nMLF), which in turn projects to the vestibular complex (Fuller, 1974), and to nIII. This represents one pathway from LcPt into the vestibular -ocular system, via the AOS, which may participate in the mediation of OKN. Montgomery (1981), suggests that three possible pathways could account for visual and vestibular integration, such as that demonstrated by Maeda, et al., (1977), in spinal motoneurons, through

(2) pretecto-bulbar, or (3) nBOR axons. A curious descending projection pattern appears through the nucleus of the posterior commissure, which in this study has been shown to project to the LcPt, and has been shown to project to the spinal cord in toads (Corraja and Ascanio, 1981). Also, the striatum projects to the nucleus reticularis tegmenti (Wilczynski and Northcutt, 1979); input to nRT also comes from LcPt (Fig. 6). This represents a possible interface between visual and somatic systems. Second-order visual units in optic tectum which have both somatic and visual input have been previously described (cf. Fite, 1969). Another projection which has counterparts in the mammalian NOT projection system comes from Pv and Pd, which project to the nucleus raphe, the analogous structure to the inferior olive (Larsell, 1967), and which has shown to receive input from NOT cells in mammals (Hoffmann, et al., 1976).

In summary, the LcPt, while demonstrating a direct projection to the region of nVI, appears to be involved in a visuomotor integration system through the interconnections with nBOR and TeO. A schematic diagram showing the interconnections between LcPt and other brain regions is shown in Figure 36. It should be noted that the cerebellum projects to peri-nBOR through the nucleus cerebelli. Connections with an oculomotor system appear with the nBOR connection, through the nMLF. Thus, LcPt not only has direct retinal input, but is interconnected with both second-order visual and motor integration systems. In the frog, both visual and vestibular information reaches spinal cord motoneurons (Maeda, et al., 1977). Spinal cord neurons

have also been observed which were both directionally and non-directionally selective to moving random-noise visual stimuli or body rotation (Ansorge and Grüsser-Cornehls, 1980). Thus, input to motoneurons through the vestibular system appear to be selective to moving visual stimuli. Input to this system could be conveyed through either nBOR, Pv, or TeO, or combinations of each.

Optokinetic nystagmus. Optokinetic nystagmus (OKN) consists of pursuit or tracking movements of the head and eyes in response to a moving stimulus pattern across the field of view, followed by an involuntary saccade in the opposite direction which enables the fixation of new contours just entering the visual field. In addition to being of particular interest as a universally observed visuomotor response, OKN can also be used as an index of various other visual functions, such as motion perception in clinical cases (Schor and Levi, 1980; Van Vliet and Van Lith, 1979), contrast sensitivity (Korner and Schiller, 1972), and visual acuity (cf. Manteuffel and Himstedt, 1978). In afoveate animals such as the rabbit, cat, and frog, stimulation of one eye elicits an asymmetric response when the stimulus is moving in the temporal-nasal direction. It has been demonstrated in cats that there is no major difference between the ipsilateral and contralateral retinal input mediating horizontal OKN (hOKN) (Precht, et al., 1980). Directional selectivity appears to be a property of units which are responsive to OKN stimulus patterns

(Collewijn, 1975), but this does not imply that the OKN system necessarily contains directionally-selective units. Several units in the present study were sensitive to the orientation of the OKN stimuli, and were not directionally-selective. A few units in PtG were more sensitive to OKN stimulus movement in the temporal-nasal direction than to any other direction. In Lpd, units were most sensitive to ventral-dorsal or nasal-temporal stimulus movement. Previous studies have only described differences in the response to hOKN vs. vertical OKN (vOKN), and did not report asymmetric properties within either hOKN or vOKN (Katte and Hoffmann, 1980). Thus, units which may be involved in the mediation of OKN may have asymmetric response properties to OKN stimulus movement in either vertical or horizontal directions.

In order to process information about motion of a stimulus, units must be responsive to stimulus movement in the visual field and not just to fixed or stationary stimuli. All but one unit in the present investigation were more responsive to moving stimuli than to stationary objects, and this has often been reported for other visual areas in the frog. The role of the LcPt in visuomotor information processing could not be clearly ascertained in the present study, due to the small sample size of the recorded units. It should be noted, however, that only two out of eight units recorded throughout the pretectal region which were responsive to moving OKN stimuli were also direction-selective, unlike previous reports (Cochran, et al., 1980; Katte and Hoffman, 1980). Units from LcPt which were

responsive to OKN stimulation showed both 'on'-'off' and 'following' types of responses to slow velocities (10°/sec) of the OKN stimulus. PtG units, however, showed response to higher stimulus velocities (25°/sec).

The fact that the presence of a moving OKN stimulus pattern at specific velocities resulted in a decrease in the spontaneous activity of three PtG units, may indicate the presence of an inhibitory mechanism in the OKN system. It should be noted that Katte and Hoffmann, (1980), found units rostral to PtG which responded to OKN stimuli by increasing their rate of sustained activity. The presence of an inhibitory mechanism in PtG is also supported by the observation that lesions of PtG resulted in an increase in the frequency of saccades, at all velocities of stimulus movement (Fite, unpublished data). The finding that lesion of either LcPt or Pd and Pv leads to disruption of the OKN response (Montgomery, et al., in press) may indicate that more rostral regions act as input to or facilitators of the OKN response, while regions caudal to LcPt could inhibit or modulate the response to OKN stimulation. It should be noted that from the same study, lesions in the anterior thalamic region corresponding to the region of retrogradely HRP-labeled cells in the nucleus rotundus (Fig. 23A) following HRP injection into LcPt (case #21), also resulted in an increase in the frequency of OKN saccades, at all velocities.

It appears that the units described here are but a sample of the different types reported in other studies, although most studies have

not reported a unit's response to a single moving contour in addition to the large-field stimuli. Such information could be relevant to whether or not the mechanism underlying OKN stimulus processing is linear. One study (Gaillard and Galand, 1979), did not find a large number of spontaneously active thalamic units, but did report responses to large-field stimuli, similar to the present study.

Single units from the pretectal region did not appear to have extremely rapid firing rates to any condition of stimulation, making it difficult to determine the 'optimal' stimulus as conventionally defined. Differences (approximately ±10%), in the response rate following different stimuli in the frog are often much less than the differences in response rate following stimulation in the mammalian central nervous system, which may be five to ten times as great (cf. Collewijn, 1975). The response differences reported in the present study have a maximum variation of ±5 spikes/sec between successive stimulus presentations, for the higher response rates, around 20 spikes/sec. The response rates observed in the present study appear to be typical of second-order units in the frog central visual system. Tectal and optic nerve fiber response rates range on the order of 5-80 spikes/sec, with typical rates around 35-40 spikes/sec (cf. Grüsser and Grüsser-Cornehls, 1976). Second-order thalamic units, however, respond with a rate from 1-30 spikes/sec, with the typical rate falling between 5 and 20 spikes/sec (cf. Fite, 1969; Brown and Marks, 1977; Gaillard and Galand, 1979; and Katte and Hoffmann, 1980). In the present study, units generally responded

with rates from 1 to 20 spikes/sec.

It is possible that units in LcPt receive tectal input, on the basis that large-field binocular neurons receiving tectal inputs have been found in caudal thalamic regions (Brown and Ingle, 1973). Furthermore, T_1, T_4, and T_6 neurons of the tectum have similar properties to those described in the present study (Grüsser and Grüsser-Cornehls, 1976). Highly directionally-selective units are not found in the optic terminal regions of the optic tectum, although there were some directionally-selective (type 3) ganglion cells reported in the retina (Grüsser and Grüsser-Cornehls, 1976). Both class 3 and class 4 ganglion cells were reported as projecting to the pretectum, although it was not clear what region was implied by the use of the term 'pretectum'. Class 3 cells respond as 'on'-'off' units, to a small object (6°-10°) moving through the receptive field. Class 4 neurons are 'off' units, or 'dimming' detectors having relatively large receptive fields (10°-15°). One unit recorded in Lpd had similar response properties to class-3 ganglion cells, and several units recorded from the anterior margin of rostral optic tectum had similar response properties to class-4 ganglion cells. This suggests that these recordings were probably from optic fibers and not from postsynaptic cells. Binocular response properties originate postsynaptic to optic tract fibers, and represent a combination of afferents to LcPt reported in the present study. Binocular neurons with receptive fields of 60°-120° have already been recorded in the frog CNS (Fite, 1969; Liege and Galand, 1972; Brown

and Ingle, 1973; Brown and Marks, 1977; and Grüsser and Grüsser-Cornehls, 1976). In addition, sensitivity to motion and 'on'-'off' responses to ambient light were found to be common features of thalamic neurons (Gaillard and Galand, 1979), consistent with the present study.

Suggestions for further research. Of prime importance is the continued investigation of response properties of single units in the various nuclei in the frog pretectal region, in order to determine response types which may be associated with particular nuclei and neuropil. The present research suggests that units in both LcPt and PtG are involved in the mediation of OKN, and the varying responses to other visual stimuli may suggest involvement of these nuclei in a variety of visually-guided behaviors. Rostral-caudal differences noted here and in the Katte and Hoffmann (1980), study, should also be examined further. Stimuli must be carefully chosen to optimize the amount of data obtainable on any given unit, considering the temporal and physiological constraints on extracellular recording in the frog central visual system.

The present study identified several units in the PtG region which were responsive to OKN stimulation, perhaps in an inhibitory manner. Since the interconnections of PtG with other brain regions have not been established, the source of this responsiveness remains ambiguous. Injections of HRP into PtG should further clarify the

pathways involved in producing the OKN responses. In addition to PtG, the connections observed between LcPt and the optic tectum could be examined through the analysis of retrograde and anterograde transport of HRP following small injections throughout the optic tectum, confirming the exact interconnection sites between the optic tectum and LcPt. These injections would also verify the apparent lack of pretectal efferents from the caudal-medial optic tectum.

The results of the present study indicate that the rationale for selecting the frog visual system as a model for neurobiological studies should not be based solely on a criterion of relative biological simplicity. Indeed, there does appear to be a high level of complexity in the frog visual system, exemplified in the present study by both the number of interconnections between the large-celled pretectal nucleus and other brain regions, and the diversity of extracellularly recorded responses from the pretectal region. Furthermore, the degree of behavioral simplicity shown by anurans is not clearly reflected by a similar simplicity of brain organization. The high level of complexity found in the mammalian brain involves large numbers of nuclei and neuropils, as well as the presence of a greatly expanded telencephalon and cortex. The smaller number of brain regions in the amphibian show a similar degree of complexity which is based on the degree of interconnections rather than on the number of associated regions. The use of the term 'model' in future research on the frog visual system should not be based upon an assumption that one is studying just a simplified version of a more

complex system. Such investigations will involve the analysis of a highly developed and specialized system, which can take advantage of the relative behavioral simplicity of anurans in anatomical and ablation studies. These studies should continue to provide insight into the understanding of general principles of brain organization.

REFERENCES

Abols, I.A. and Basbaum, A.I. The posterior pretectal nucleus: evidence for a direct projection to the interior olive of the cat. Neurosci. Letters, 13, 1979, 111-116.

Ansorge, K. and Grüsser-Cornehls, U. Neurons in the spinal cord of the frog responding to moving visual stimuli. Neurosci. Letters, 18, 1980, 53-58.

Baarsma, E.A. and Collewijn, H. Vestibulo-ocular and optokinetic reactions to rotation and their interaction in the rabbit. J. Physiol. (Lond.), 238, 1974, 603-625.

Ballas, I., Hoffmann, K.P. and Wagner, H.-J. Retinal projection to the nucleus of the optic tract in the cat as revealed by retrograde transport of horseradish peroxidase. Neurosci. Letters, 26, 1981, 197-202.

Bellonci, J. Uber die centrale Endiguing des nervus Opticus bei den Vertebraten. Zeitsch. f. Wissensch. Zool., B.d., 47, 1888 51.

Benevento, L.A., Rezak, M. and Santos-Anderson, R. An autoradiographic study of the projection of the pretectum in the rhesus monkey (Macaca mulatta): Evidence for sensorimotor links to the thalamus and occulomotor nuclei. Brain Res., 127, 1977, 197-218.

Berlucchi, G., Sprague, J.M., Levy, J., DiBerardino, A.C. Pretectum and superior colliculus in visually guided behavior and in flux and form discrimination in the cat. J. Comp. Physiol.

Monographs, 78, 1972, 123-172.

Berman, N. Connections of the pretectum in the cat. J. Comp. Neurol., 174, 1977, 227-254.

Blair, W.F. Amphibians, their evolutionary history, taxonomy, and ecological adaptations, in The Amphibian Visual System: A Multidisciplinary Approach, Fite, K.V. (Ed.) Academic Press, New York, 1976, 1-24.

Bon, L., Corazza, R. and Inchingolo, P. Neuronal activity correlated with eye movement in cat's pretectum. Neurosci. Letters, 5, 1977, 69-74.

Brown, W.T. and Ingle, D. Receptive field changes produced in frog thalamic units by lesions of the optic tectum. Brain Res., 59, 1973, 405-409.

Brown, W.T. and Marks, W.B. Unit Responses in the frog's caudal thalamus. Brain Behav. Evol. 14, 1977, 274-297.

Carey, R.G. A quantitative analysis of the distribution of the retinal elements in frogs and toads with special emphasis on the area retinalis. Unpublished masters thesis, University of Massachusetts, Amherst, MA, 1975.

Carpenter, H.R.S. Cerebellectomy and the transfer function of the vestibulo-ocular reflex in the decerebrate cat. Proc. roy. Soc. B, 181, 1972, 353-374.

Carpenter, M.B. and Pierson, R.J. Pretectal region and pupillary light reflex: An anatomical analysis in the monkey. J. Comp. Neurol., 149, 1973, 271-300.

Carterette, E.C. and Friedman, M.P. (Eds.) Handbook of Perception Vol. V. Seeing. Academic Press, New York, 1975, p. 49.

Cochran, S.L., Precht, W. and Dieringer, N. Direction-selective neurons in the frog's visual system. Soc. Neurosci. Abstr., 6, 1980, 121.

Collewijn, H. Direction-selective units in the rabbit's nucleus of the optic tract. Brain Res., 100, 1975, 489-508.

Collewijn, H. Eye- and head movements in freely moving rabbits. J. Physiol. 266, 1977, 471-498.

Collewijn, H. and Kleinschmidt, H.J. Vestibulo-ocular and optokinetic reactions in the rabbit: changes during 24 hours of normal and abnormal interaction. In Basic Mechanisms of Ocular Motility and their Clinical Interpretations, Lennerstrand, G. and Bach-y-Rita (Eds.), Pergamon Press, Oxford. 1975, 477-483.

Corraja, N. and Ascanio, P. Spinal projections from the mesencephalon in the toad. Brain, Behav. Evol., 19, 1981, 205-213.

Currie, J.R. and Cowan, W.M. Evidence for the late development of the uncrossed retino-thalamic projections in the frog Rana pipiens. Brain Res., 71, 1974, 133-139.

Dowben, R.M. and Rose, J.E. A metal filled microelectrode. Science, 118, 1953, 22.

Dubois, M.F.W. and Collewijn, H. The optokinetic reactions of the rabbit: relation to the visual streak. Vis., Res., 19, 1979, 9-17.

Dufossé, M., Ito, M. Jastreboff, P.J. and Miyashita, Y. A neuronal correlate in rabbits' cerebellum to adaptive modification of the vestibulo-ocular reflex. Brain Res. 150, 1978, 611-616.

Ebbesson, S.O.E. and Meyer, D.L. The visual system of the guitar fish (Rhinobatos productus). Cell Tissue Res., 206, 1980, 243-250.

Erickson, R.G. and Barmack, N.H. A comparison of the horizontal and vertical optokinetic reflexes of the rabbit. Exp. Brain Res., 40, 1980, 448-456.

Ewert, J.-P. Neural mechanisms of prey-catching and avoidance behavior in the toad (Bufo bufo L.). Brain Behav. Evol., 3, 1970, 36-56.

Ewert, J.-P. Single unit response of the toad's (Bufo americanus) caudal thalamus to visual objects. A. vergl. Physiol., 74., 1971, 81-102.

Ewert, J.-P. The visual system of the toad: Behavioral and physiological studies on a pattern recognition system. In: The Amphibian Visual System (ed. K.V. Fite), pp. 141-202. New York, Academic Press, 1976.

Ewert, J.-P. and von Wietersheim, A. Pattern analysis by tectal and thalamus/pretectal nerve nets in the visual system of the toad (Bufo bufo L.). J. Comp. Physiol., 92, 1974a, 131-148.

Ewert, J.-P and von Wietersheim, A. Influence of thalamus/pretectal lesions on the response of tectal neurons to visual objects in the toad (Bufo bufo L.). J. Comp. Physiol., 92, 1974b, 149-160.

Ewert, J.-P., Hock, F.J. and von Wietersheim, A. Thalamus, pretectum, tectum: retinal topography and physiological interactions in the toad (Bufo bufo L.). J. Comp. Physiol., 92, 1974, 343-356.

Fite, K.V. Single-unit analysis of binocular neurons in the frog optic tectum. Exp. Neurol., 24, 1969, 475-486.

Fite, K.V. The visual fields of the frog and toad: A Comparative Study. Behav. Biology, 9, 1973, 707-718.

Fite, K.V. (Ed.) The Amphibian Visual System: A Multidisciplinary Approach, Academic Press, New York, 1976.

Fite, K.V., Carey, R.G. and Vicario, D. Visual neurons in frog anterior thalamus. Brain Res., 127, 1977, 283-290.

Fite, K.V., Soukup, J. and Carey, R.G. Wavelength discrimination in the leopard frog: A reexamination. Brain Behav. Evol., 15, 1978, 404-414.

Finkenstadt, Th. Disinhibition of prey-catching in the salamander following thalamic-pretectal lesions. Naturwissenschaften, 67, 1980, 471.

Fuller, P.M. Projections of the vestibular nuclear complex in the bullfrog (Rana catesbeiana). Brain Behav. Evol., 10, 1974, 157-169.

Gaillard, F. and Galand, G. Diencephalic binocular wide field neurons in the frog. Exp. Brain Res., 34, 1979, 511-520.

Gaze, R.M. and Keating, M.J. Receptive field properties of single units from the visual projection to the ipsilateral tectum in the frog. Quart. J. Exp. Physiol., 55, 1970, 143-152.

Goldberg, S. and Kotani, M. The projection of optic nerve fibers in the frog Rana catesbiana as studied by autoradiography. Anat. Rec., 158, 1967, 325-332.

Grahm, J. and Berman, N. Origins of the pretectal and tectal projections to the central lateral nucleus in the cat. Neurosci. Letters, 26, 1981, 209-214.

Grover, B.G. and Sharma, S.C. Organization of extrinsic tectal connections in goldfish (Carassius auratus). J. Comp. Neurol., 196, 1981, 471-478.

Grüsser, O.-J. and Grüsser-Cornehls, U. Neurophysiology of the anuran visual system. In: Frog Neurobiology (Eds. R. Llinas, W. Precht), pp. 297-385. New York: Springer, 1976.

Grüsser, O.-J., Pause, M. and Schreiter, U. Three methods to elicit sigma-optokinetic nystagmus in Java monkeys. Exp. Brain Res., 35, 1979, 519-526.

Hall, W.C. and Ebner, F.F. Parallels in the visual afferent projections of the thalamus in the hedgehog (Paraechinus hypomelas) and the turtle (Pseudemys scripta). Brain Behav. Evol., 3, 1970, 135-154.

Hanker, J.S., Yates, P.E., Metz, C.B., and Rustioni, A. A new specific, sensitive and non-carcinogenic reagent for the demonstration of horseradish peroxidase. Histochem. J., 9, 1977, 789-792.

Harris, L.R., Leporé, F., Guillemot, J.-P. and Cynader, M. Abolition of optokinetic nystagmus in the cat. Sci., 210, 1980, 91-92.

Hartline, H.K. The nerve messages in the fibers of the visual pathway. J. Opt. Soc. Amer., 30, 1940, 239-247.

Hepp, K., Henn, V. and Jaeger, J. Eye movement related neurons in the cerebellar nuclei of the alert monkey. Exp. Brain Res., 45, 1982, 253-264.

Herrick, C.J. The amphibian forebrain. III. The optic tracts and centers of amblystoma and the frog. J. Comp. Neurol., 39, 1925, 433-489.

Hertzler, D.R. Tectal integration of visual input in the turtle. Brain Behav. Evol., 5, 1972, 240-255.

Hertzler, D.R. and Hayes, W.N. Cortical and tectal function in visually guided behavior of turtles. J. Comp. Physiol. Psych., 63, 1967, 444-517.

Hodos, W. The concept of homology and the evolution of behavior. In: Masterson, R.B., Hodos, W. and Jerison, H. (Eds.) Evolution, Brain, and Behavior: Persistent Problems. John Wiley and Sons, New York, 1976.

Hoffmann, K.-P., Behrend, K. and Schoppmann, A. A direct afferent visual pathway from the nucleus of the optic tract to the inferior olive in the cat. Brain Res., 115, 1976, 150-153.

Hoffman, K.-P. and Schoppmann, A. A quantative analysis of the direction-specific response of neurons in the cat's nucleus of the optic tract. Exp. Brain Res., 42, 1981, 146-157.

Ingle, D. Disinhibition of tectal neurons by pretectal lesions in the frog. Science, 180, 1973a, 422-424.

Ingle, D. Two visual systems in the frog. Science, 181, 1973b, 1053-1055.

Ingle, D. Behavioral correlates of central visual function in Anurans. In: Frog Neurobiology, Eds. R. Llinás, W. Precht. New York: Springer-Verlag, 1976.

Ingle, D. Detection of stationary objects by frogs following optic tectum ablation. J. Comp. Physiol. Psychol., 91, 1977, 1359-1364.

Ingle, D. Some effects of pretectum lesions on the frog's detection of stationary objects. Behav. Brain Res., 202, 1981, 265-285.

Itoh, K. Efferent projections of the pretectum in the cat. Exp. Brain Res., 30, 1977, 89-106.

Kanaseki, T. and Sprague, J.M. Anatomical organization of pretectal nuclei and tectal laminae in the cat. J. Comp. Neurol., 158, 1974, 319-338.

Katte, O. and Hoffmann, K.-P. Direction specific neurons in the pretectum of the frog (Rana esculenta). J. Comp. Physiol. A, 140, 1980, 53-57.

Kemali, M. and Braitenberg, V. Atlas of the Frog's Brain. 74p. New York, Springer, 1969.

Kicliter, E. Flux, wavelength, and movement discrimination in frogs: forebrain and midbrain contributions. Brain Behav. Evol, 8, 1973, 340-365.

Knapp, H., Scalia, F. and Riss, W. The optic tracts of Rana pipiens. Acta Neurol. Scandinav., 41, 1965, 325-355.

Korner, F. and Schiller, P.H. The optokinetic response under open and closed loop conditions in the monkey. Exp. Brain Res., 14, 1972, 318-330.

Larsell, O. The development of the cerebellum in the frog (Hyla regilla). J. Comp. Neurol., 39, 1967, 249-289.

Lázár, Gy. and Székely, Gy. Distribution of optic terminals in the different optic centers of the frog. Brain Res., 16, 1969, 1-14.

Lázár, G. Role of the accessory optic system in the optokinetic nystagmus of the frog. Brain Behav. Evol., 5, 1973, 443-460.

Lázár, G. Application of cobalt-filling technique to show retinal projections in the frog. Neuroscience, 3, 1978, 725-736.

Legg, C.R. Do pretectal lesions impair visual discrimination acquisition in rats? Physiol. Behav., 18, 1977, 781-786.

Lettvin, J.Y., Maturana, H.R., McCulloch, W.S. and Pitts, W.H. What the frog's eye tells the frog's brain. Proc. Inst. Radio Engrs., 47, 1959, 1940-1951.

Levine, R.L. An autoradiographic analysis of the retinal projection in the frog Xenopus laevis: new observations in an anuran visual projection. Brain Res., 148, 1978, 202-206.

Levine, R.L. An autoradiographic study of the retinal projection in Xenopus laevis with comparisons to Rana. J. Comp. Neurol., 189, 1980, 1-29.

Liege, B. and Galand, G. Single unit visual responses in the frog's brain. Vision Res., 12, 1972, 609-622.

Llinás, R. and Precht, W. (Eds.) Frog Neurobiology: A Handbook. Springer-Verlag. New York, 1976.

Maeda, M., Magherrini, P.C. and Precht, W. Functional organization of vestibular and visual inputs to neck and forelimb motoneurons in the frog. Exp. Brain Res., 29, 1977, 225-243.

Maekawa, K. and Kimura, M. Electrophysiological study of the nucleus of the optic tract that transfers optic signals to the nucleus reticularis tegmenti pontis - the visual mossy fiber pathway to the cerebellar flocculus. Brain Res., 211, 1981, 456-462.

Manteuffel, G.M. and Himstedt, W. The aerial and aquatic visual activity of the optomotor response in the crested newt (Triturus cristatus). J. Comp. Physiol. A., 128, 1978, 359-365.

Mayr, E. Behavior and Systematics. In Behavior and Evolution. Roc, A. and Simpson, G.G. (Eds.). New Haven: Yale University Press, 1958.

Miles, F.A. and Fuller, J.H. Adaptive plasticity in the vestibulo-ocular responses in the rhesus monkey. Brain Res., 80, 1974, 512-516.

Montarolo, P.G., Precht, W. and Strata, P. Functional organization of the mechanisms subserving the optokinetic nystagmus in the cat. Neurosci., 6, 1981, 231-246.

Montgomery, N. Visuo-motor connections in the anuran mesencephalon. Master of Science Thesis, Psychology, University of Massachusetts, Amherst, MA, 1981.

Montgomery, N., Fite, K.V. and Bengston, L. The accessory optic system of Rana pipiens: Neuroanatomical connections and intrinsic organization. J. Comp. Neurol., 203, 1981, 595-612.

Montgomery, N., Fite, K.V., Taylor, M., and Bergston, L. Neural correlates of optokinetic nystagmus in the mesencephalon of Rana pipiens: A functional analysis, Brain, Behav. Evol., in press.

Mori, J., Hori, N. and Katsuda, N. A new method for application of horseradish peroxidase into a restricted area of the brain. Brain Res. Bulletin, 6, 1981, 19-22.

Muntz, W.R.A. Effectiveness of different colors of light in releasing the positive phototaxic behavior of frogs, and a possible function of the retinal projection to the diencephalon. J. Neurophysiol., 25, 1962, 712-720.

Neary, T.J. Architectonics of the thalamus of the bullfrog (Rana catesbieana): A histochemical analysis. Anat. Rec., 181, 1975, 434.

Neary, T.J. An autoradiographic study of retinal projections in some members of 'archaic' and 'advanced' anuran families. Anat. Rec., 184, 1976, 487.

Neverov, V.P., Sterc, J. and Bures, J. Electrophysiological correlates of the reversed postoptokinetic nystagmus in the rabbit: Activity of vestibular and floccular neurons. Brain Res., 189, 1980, 355-367.

Nieuwenhuys, R. and Opdam, P. Structure of the brain stem. In R. Llinás and W. Precht (Eds.): Frog Neurobiology. Berlin: Springer-Verlag, 1977, pp. 407-434.

Pasik, P. and Pasik, T. Oculomotor functions in monkeys with lesions of the cerebrum and superior colliculi; The Oculomotor System. Harper and Row, New York, 1964.

Pasik, T., Pasik, P. and Bender, M.B. The pretectal syndrome in monkeys: II. Spontaneous and induced nystagmus and 'lighting' eye movement. Brain, 92, 1977, 871-884.

Precht, W., Montarolo, P.G. and Strata, P. The role of the crossed and uncrossed retinal fibers in mediating the horizontal optokinetic nystagmus in the cat. Neurosci. Letters, 17, 1980, 39-42.

Reperant, J., Rio. J.-P. and Amouzou, M. Radiographic analysis of the retinofugal pathways in the primitive bony fish, Polypterus senegalus. C.R. Hegd. Seances. Acad. Sci. Ser. D. Sci. Nat., 289, 1979, 947-950.

Reuter, T. and Virtanen, K. Border and colour coding in the retina of the frog. Nature (London), 239, 1972, 260-263.

Robertson, R.T., Kaitz, S.S. and Robards, M.J. A subcortical pathway links sensory and limbic systems of the forebrain. Neurosci. Letters, 17, 1980, 161-166.

Rubinson, K. Projections of the tectum opticum of the frog. Brain Behav. Evol., 1, 1968, 529-561.

Scalia, F., Knapp, H., Halpern, M. and Riss, W. New observations in the retinal projection in the frog. Brain Behav. Evol., 1, 1968, 324-353.

Scalia, F. and Gregory, K. Retinofugal projections in the frog: Location of the postsynaptic neurons. Brain Evol. Behav., 3, 1970, 16-29.

Scalia, F. and Colman, D.R. Aspects of the central projection of the optic nerve in the frog revealed by anterograde migration of H.R.P. Brain Res., 79, 1974, 496-504.

Scalia, F. and Fite, K.V. A retinotopic analysis of the central connections of the optic nerve in the frog. J. Comp. Neurol., 158, 1974, 455-478.

Scalia, F. The optic pathway of the frog: Nuclear organization and connections. In: Frog Neurobiology, Eds. R. Llinas, W. Precht. New York: Springer-Verlag, 1976.

Scalia, F. and Arango, V. Topographic organization of the projections of the retina to the pretectal region in the rat. J. Comp. Neurol., 186, 1979, 271-292.

Schoppmann, A. and Hoffmann, K.-P. A comparison of visual responses in two pretectal nuclei and in the superior colliculus of the cat. Exp. Brain Res., 35, 1979, 495-510.

Schor, C.M. and Levi, D.L. Disturbances of small field horizontal and vertical optokinetic nystagmus in amblyopia. Invest Opthalmol. Visual Sci., 19, 1980, 688-694.

Simpson, J.I., Soodak, R.E. and Hess, R. The accessory optic system and its relation to the vestibulo cerebellum. In Reflex Control of Posture and Movement. Granit, R. and Pompeiano, O. (Eds.) Progress in Brain Res., 50, 1979, Elsevier, North Holland.

Steedman, J.G., Stirling, R.V., and Gaze, R.M. The central pathways of optic fibers in Xenopus tadpoles. J. Embryol. Exp. Morph., 50, 1979, 199-215.

Stone, J. The Wholemount Handbook, Maitland Publications Pty., Ltd., 1981.

Székely, G. The mesencephapic and diencephalic optic centers in the frog. Vision Res. Supplement, #3, 1971, 269-279.

Székely, G. and Lázár, Gy. Cellular and synaptic architecture of the optic tectum in Frog Neurobiology, A handbook, Llinás, R. and Precht, W. (Eds.), Springer-Verlag, New York, 1976, 407-434.

Thoden, V., Dichgans, J., Doerr, M., and Savides, T. Direction specific vestibular and visual modulation of fore-and hind limb reflexes in cats. In Reflex Control of Posture and Movement. Granit, R. and Pompeiano, O. (Eds.) Progress in Brain Research, 50, 1979, 211-218.

Trachtenberg, M.C. and Ingle, D. Thalamo-tectal projections in the frog. Brain Res., 79, 1974, 419-430.

Van Vliet, A.G.M. and Van Lith, G.H.M. Nystagmography as a diagnostic tool in multiple sclerosis. Documenta Ophtalmologica, 46, 1979, 339-344.

Vesselkin, N.P., Agayan, A.L., and Nomokonova, L.M. A study of thalamo-telencephalic afferent systems in frogs. Brain Behav. Evol., 4, 1971, 295-306.

von Wietersheim, A. and Ewert, J.-P. Neurons of the toad's (Bufo bufo L.) visual system sensitive to moving configurational stimuli: A statistical analysis. J. Comp. Physiol., 126, 1978, 35-42.

Weber, J.T. and Harting, J.K. The efferent projections of the pretectal complex: An autoradiographic and horseradish peroxidase analysis. Brain Res., 194, 1980, 1-28.

Weber, J.T. and Hutchins, B. The demonstration of a retinal projection to the medial pretectal nucleus in the domestic cat and the squirrel monkey: an autoradiographic analysis. Brain Res., 232, 1982, 181-186.

Wilczynski, W. and Northcutt, R.G. Afferents to the optic tectum of the leopard frog: An HRP study. J. Comp. Neurol., 173, 1977, 219-230.

Wilczynski, W. and Northcutt, R.G. An HRP study of the anuran striatum. Anat. Rec., 193, 1979, 721.

Winterkorn, J.M.S. and Meikle, T.H. Distractibility of cats with lesions of the superior colliculus-pretectum during performance of a 4-choice visual discrimination. Brain Res., 206, 1981, 345-360.

APPENDIX A

TABLE I

Nomenclature

A	-	anterior thalamic nucleus (Neary, 1975)
Adt	-	anterodorsal tegmental nucleus (Potter, 1965)
Al	-	auricular lobe of the cerebellum (Kemali and Braitenberg, 1969)
Avt	-	anteroventral tegmental nucleus
B	-	neuropil of Bellonci
C	-	central thalamic nucleus
Cbl	-	cerebellar layers (Kemali and Braitenberg, 1969)
Cbn	-	cerebellar nucleus (Kemali and Braitenberg, 1969)
CO	-	subcommissural organ
Cg	-	corpus geniculatum thalamicum
DH	-	dorsal hypothalamus
Ec	-	contralateral descending tectal efferents (Wilczynski and Northcutt, 1977)
Ei	-	ipsilateral descending tectal efferents (Wilczynski and Northcutt, 1977)
Ep	-	posterior entopeduncular nucleus
Hd	-	dorsal habenula
Hv	-	ventral habenula
La	-	anterior lateral thalamic nucleus
LcPt	-	large-celled pretectal nucleus
Lpd	-	posterodorsal lateral thalamic nucleus (Neary, 1975)

Lpv - posteroventral lateral thalamic nucleus

Mg - magnocellular nucleus

Mlcb - molecular layer of the cerebellum

Mlf - medial longitudinal fasciculus

mnV - motor nerve V

nIII - occulomotor nucleus

nVI - nucleus nervi abducentis (Nieuwenhuys and Opdam, 1976)

nBOR - nucleus of the basal optic root

nIp - nucleus interpeduncularis (Nieuwenhuys and Opdam, 1976)

nIs - nucleus isthmi

nMLF - nucleus of the medial longitudinal fasciculus

nIII - nucleus of the occulomotor nerve

nP - nucleus profundus

NPC - nucleus of the posterior commissure

NP - nucleus of the periventricular organ

RM - nucleus reticularis medius (Nieuwenhuys and Opdam, 1976)

Pd - posterodorsal thalamic nucleus

Pdt - posterodorsal tegmental nucleus (Potter, 1965)

Pn - posterior thalamic nucleus

PnBOR - peri-nBOR (Montgomery, et al., 1981)

PtG - pretectal gray

PtrG - pretoral gray

Pv - posteroventral thalamic nucleus

Pvt - posteroventral tegmental nucleus (Potter, 1965)

R - nucleus Rotundus

SC - suprachiasmatic area

SO - superior olive

TC - commissural nucleus of torus (Potter, 1965)

Te6 - lamina 6 of the optic tectum (Neary, 1975)

Tel - telencephalon

TeO - optic tectum

TMC - magnocellular nucleus of the torus (Potter, 1965)

TP - posterior tubercle

Tsem - subependymal nucleus of the torus (Potter, 1965)

U - uncinate

VI - abducens

VIIId - dorsal nucleus of the eighth nerve

VH - ventral hypothalamus

Vld - dorsal ventrolateral nucleus

Vlv - ventral ventrolateral nucleus

VM - ventromedial nucleus

TABLE II

Response Properties of Single Units

Unit #	Recording Site	'on'-'off'	Spon. Act.	OKN Response Type	OKN Response Vel. Range	vOKN	hOKN	R.F. Size	Binocular/ Monocular
9	LcPt	'off'	Yes	---	---	---	---	> 90°	Binocular
13		'off'-('on')	No	on-off, following	10°/sec ±2°	Yes	Yes	10°±5°	Contralateral
14		'off'-('on')	No	on-off	10°/sec ±2°	Yes	Yes	25°±5°	Binocular
10	PtG	'off'-('on')	No	---	---	---	---	30°±5°	Contralateral
17a		'on'-'off'	No	---	---	---	---	> 90°	---
17b		'off'-('on')	No	on-off, following				20°±5°	Binocular
17c		'off'-('on')	No	None	---	---	---	> 90°	Binocular
18		'on'-('off')	Yes	following	10°-50°/sec	Yes	Yes	45°±5°	Binocular
19a		'on'-'off'	Yes	on-off, following	25°/sec ±5°	Yes	Yes	---	---
19b		'on'-'off'	Yes	on, following	25°sec ±5°	Yes	Yes	30°±5°	Binocular
15	Lpd	'off'-('on')	No	on-off	10°-20°/sec	Yes	Yes	> 90°	Binocular
16a		'on'-'off'	No	None	---	---	---	50°±10°	Contralateral
16b		'on'-('off')	No	None	---	---	---	30°±10°	Contralateral
1	TeO	'off'	No	following	10°/sec	---	Yes	45°±10°	Contralateral
11		'off'-('on')	No	---	---	---	---	> 90°	Binocular
12		'off'-('on')	No	on-off	10°-25°/sec	---	Yes	30°±10°	Contralateral
8	Pd	'on'-'off'	No	---	---	---	---	---	---

APPENDIX B

Fig. 1. Drawing of the frog brain (lateral view) showing in dotted outline the posterior (P), lateral (L) and anteroventral (B, C) segments of the thalamic neuropil associated with the projections of the retina and the tectum. (B) nucleus of Bellonci; (C) corpus geniculatum thalamicum; (i) nucleus isthmi; (op) optic tract; (T) optic tectum; (x) basal optic nucleus; (S) striatum (from Scalia, 1976). Anterior is toward the right.

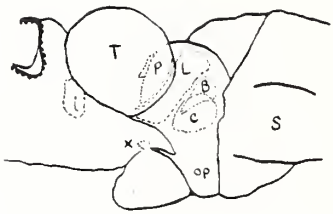

Figure 1

Fig. 2. Drawings of sections (a-f) of frog brain (R. pipiens) showing the cell-masses of the thalamus in relation to the major areas of the neuropil. (B) nucleus of Bellonci; (C) corpus geniculatum thalamicum; (L) lateral neuropil; (P) posterior thalamic nucleus; (cg) central grey; (ch) optic chiasma; (ep) posterior entopeducular nucleus; (hd) dorsal habenular nucleus; (he) ventral habenular nucleus; (hy) hypothalamus; (lg) lateral geniculate nucleus; (pc) posterocentral nucleus; (pl) posterolateral nucleus; (pp) large-celled pretectal nucleus; (pr) preoptic area; (r) nucleus rotundus; (v) posterior ventral thalamus; (vl) ventrolateral nucleus; (x) basal optic nucleus. (from Scalia, 1976)

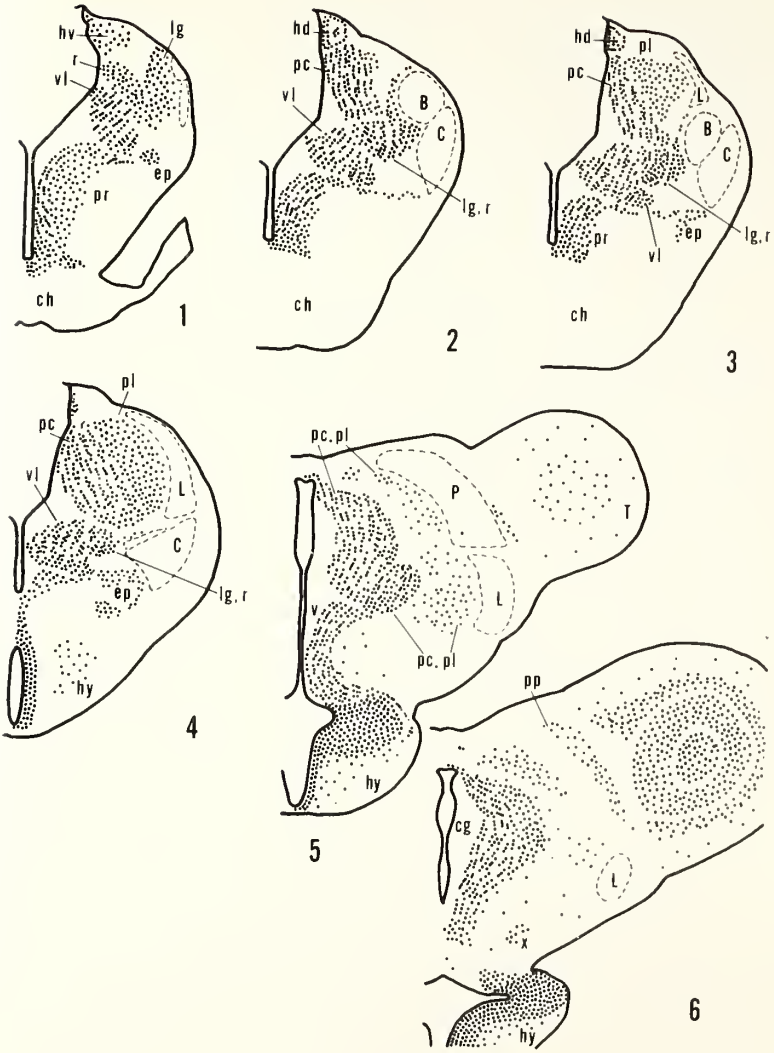
hv
lg
r
vl
ep
pr
ch
1
hd
pc
vl
B
C
lg, r
ch
2
hd
pl
pc
L
B
C
pr
vl
ep
lg, r
ch
3
pl
pc
vl
L
C
ep
lg, r
hy
4
pc, pl
P
T
L
v
pc, pl
hy
5
pp
cg
L
x
hy
6

Fig. 3 Top. A schematic drawing of a coronal section through the telencephalon of the leopard frog, Rana pipiens, showing the major cell nuclei. The dashed line represents a fiber labeled with HRP following an injection into LcPt (abbreviations are given in Table I.).

Bottom. A schematic drawing of a lateral view of a Rana pipiens brain showing the relative positions of the numbered coronal sections presented in Figures 3-8, inclusive. Bs- brainstem region; TeO - optic tectum; Th - thalamic region; Fb - forebrain.

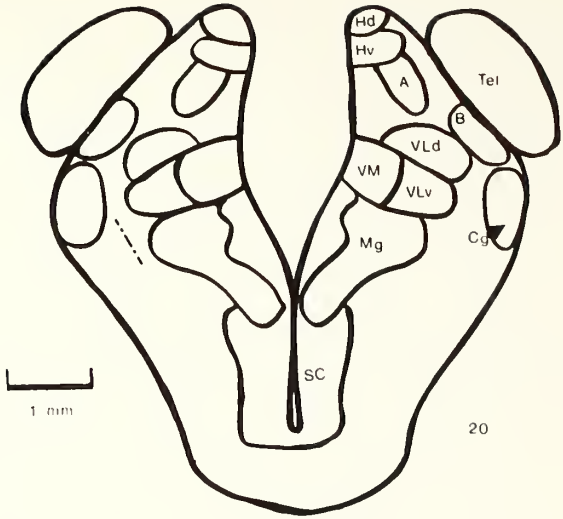
Hd
Hv
A
Tel
B
VLd
VM
VLv
Mg
Cg
SC
1 mm
20

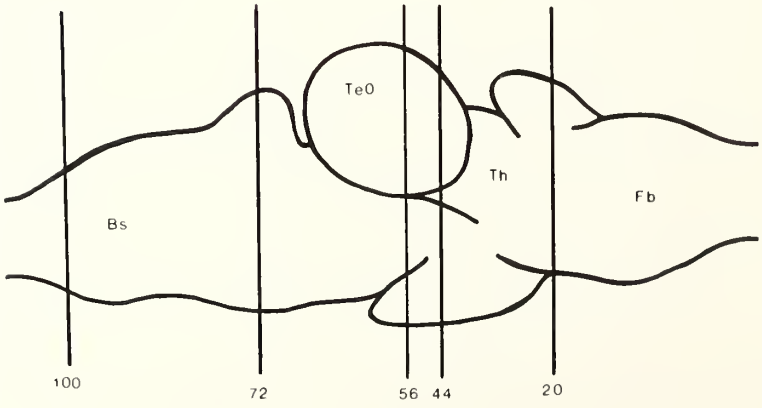
TeO
Th
Fb
Bs
100
72
56
44
20

Fig. 4. Top. Diagram of a coronal section through the anterior thalamus of Rana pipiens. Dark triangles represent HRP- labeled cells after an injection of HRP into LcPt. Nomenclature for this figure and for the following figures is given in Table I.
Bottom. A coronal section through the anterior thalamic region 400µm caudal to the top section (#28).

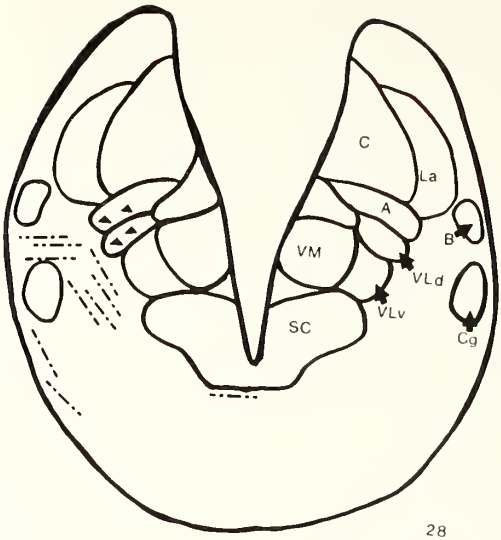

28

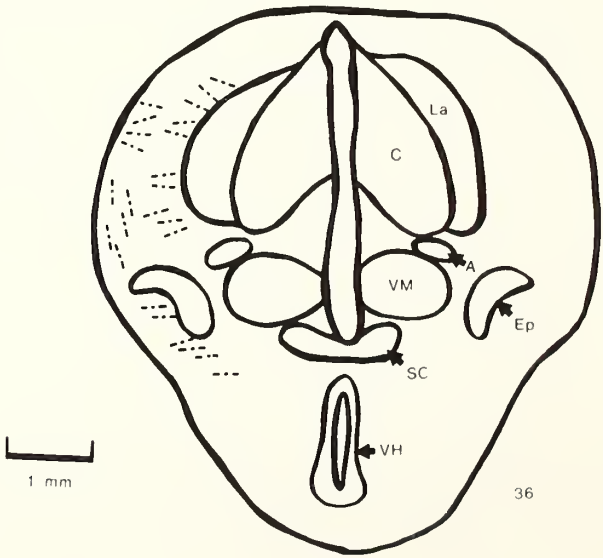

1 mm

36

Fig. 5. Top. Diagram of a coronal section through the posterior thalamic region of Rana pipiens, following HRP injection into LcPt.
Bottom. A coronal section through the meso-diencephalic region of Rana pipiens showing the location of the HRP injection site (dark ellipse) into LcPt (symbols explained in Fig. 3 and 4).

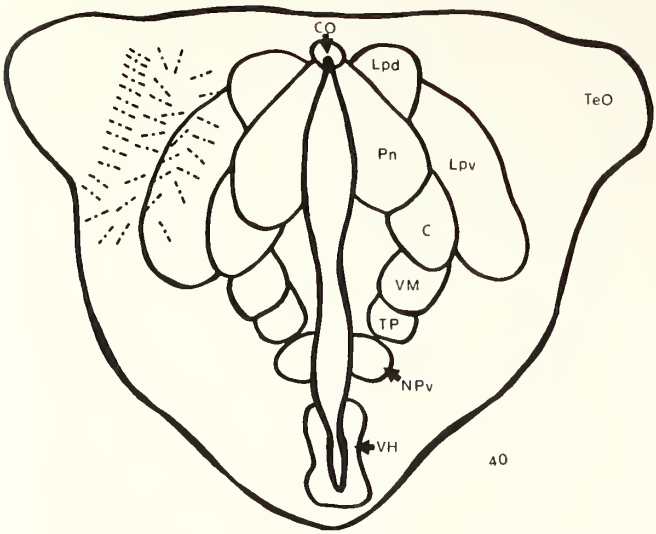
CO
Lpd
TeO
Pn
Lpv
C
VM
TP
NPv
VH
40

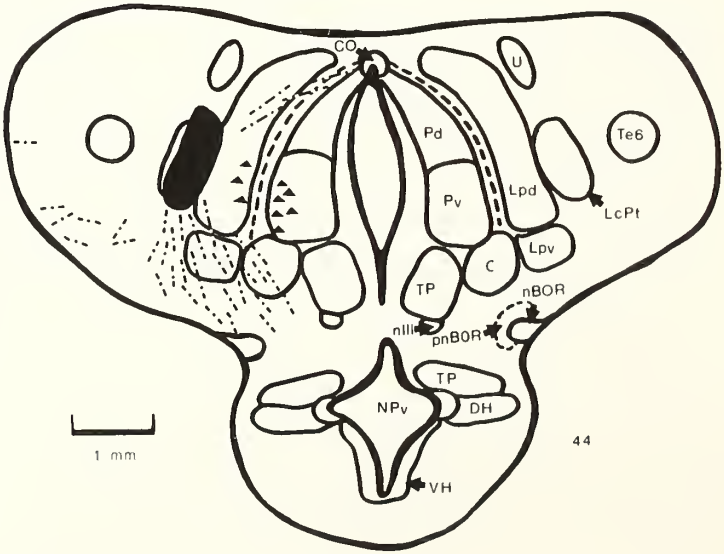
CO
U
Pd
Te6
Pv
Lpd
LcPt
Lpv
C
TP
nBOR
nIII
pnBOR
TP
NPv
DH
VH
1 mm
44

Fig. 6. Top. Diagram of a coronal section through the anterior optic tectum showing the location of fibers and cells after the HRP injection in LcPt, shown in Fig. 5.

Bottom. Diagram of a coronal section 100μm caudal to the top section (#46). Dark circles represent terminal sites following HRP injection in LcPt, shown in Fig. 5 (symbols explained in Figures 3 and 4).

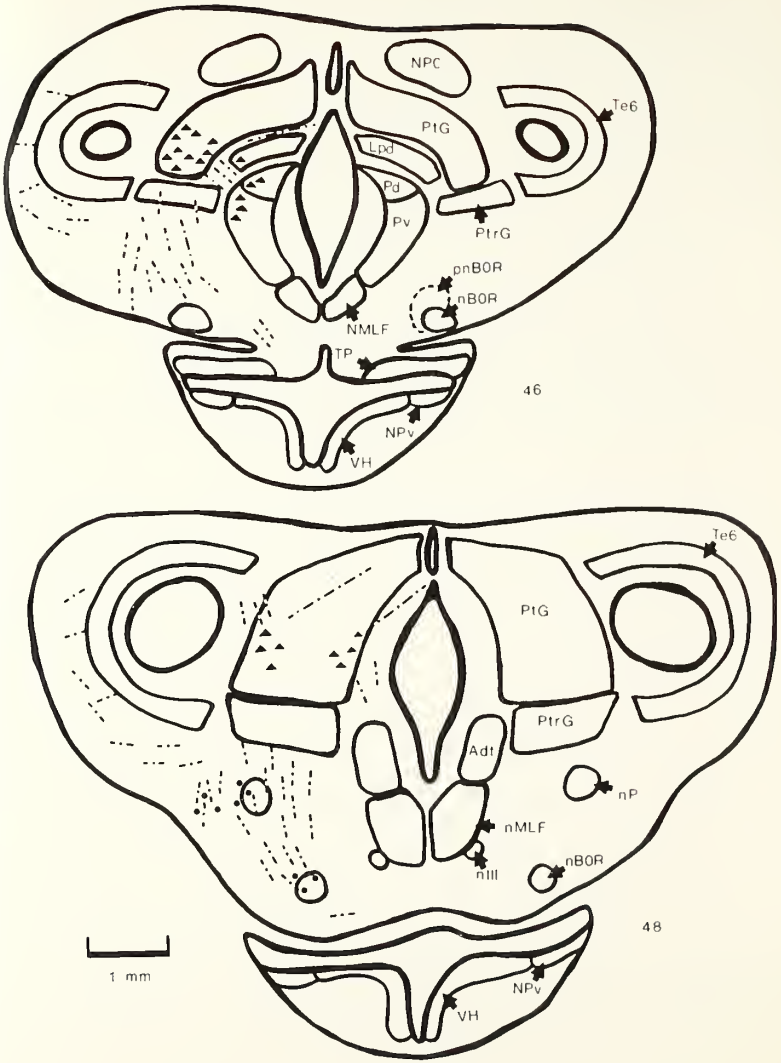
NPC
Te6
PtG
Lpd
Pd
Pv
PtrG
pnBOR
nBOR
NMLF
TP
46
NPv
VH
Te6
PtG
PtrG
Adt
nP
nMLF
nIII
nBOR
48
1 mm
NPv
VH

Fig. 7. Top. Diagram of a coronal section at the level of the torus, following the HRP injection in LcPt, shown in Fig. 5.
Bottom. Diagram of a coronal section 400μm caudal to top section (#56), following the HRP injection in LcPt, shown in Fig. 5 (symbols explained in Figures 3 and 4).

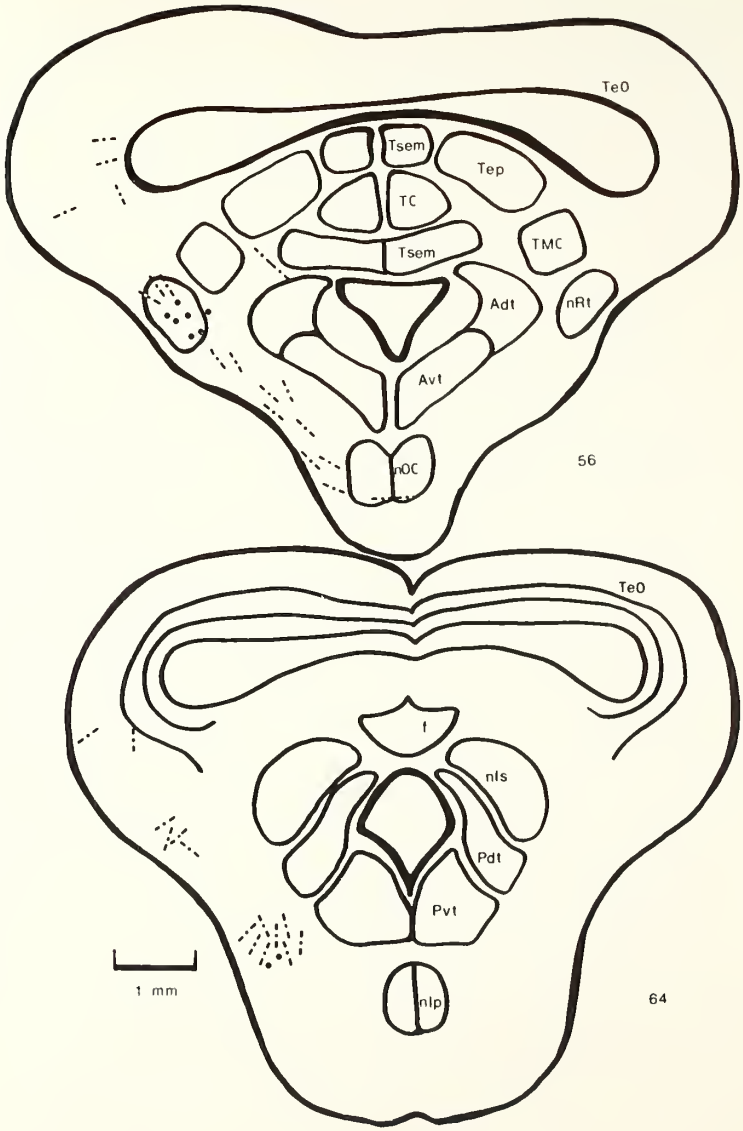
TeO
Tsem
Tep
TC
Tsem
TMC
Adt
nRt
Avt
nOC
56
TeO
I
nIs
Pdt
Pvt
nIp
1 mm
64

Fig. 8. Top. Diagram of a coronal section through the cerebellum of Rana pipiens following HRP injection in LcPt, shown in Fig. 5.

Bottom. Diagram of a coronal section through the brainstem following the HRP injection into LcPt, shown in Fig. 5. This section represents the last section containing HRP-labeled fibers (symbols are explained in Figures 3 and 4).

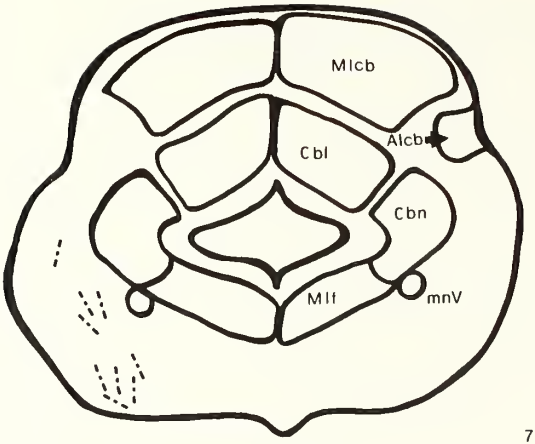

72

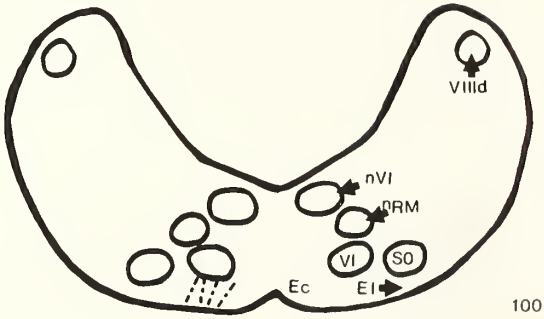

100

1 mm

Fig. 9A. Photomicrograph of a coronal section through the pretectal region showing the location of HRP injection in LcPt, case #21.

Figure 9A

Fig. 9B. A schematic representation of the injection site in Fig. 9A showing the major regions shown in the photomicrograph. This section corresponds to the coronal schematic of Fig. 5 (bottom).

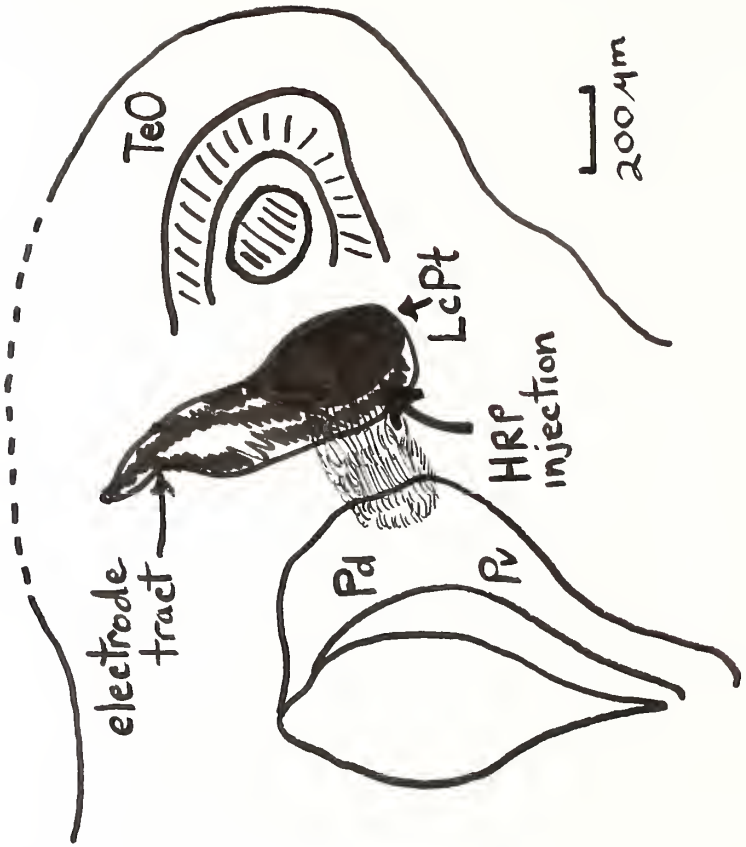

Figure 9B

Fig. 10A. Photomicrograph of a section from the central retina in Rana pipiens showing the ganglion cells retrogradely labeled, following an HRP injection confined to LcPt, (case #33).

Figure 10A

Fig. 10B. A schematic of Fig. 10A showing the location of HRP-labeled ganglion cells (G.C.) relative to the pigment epithelium (P.E.).

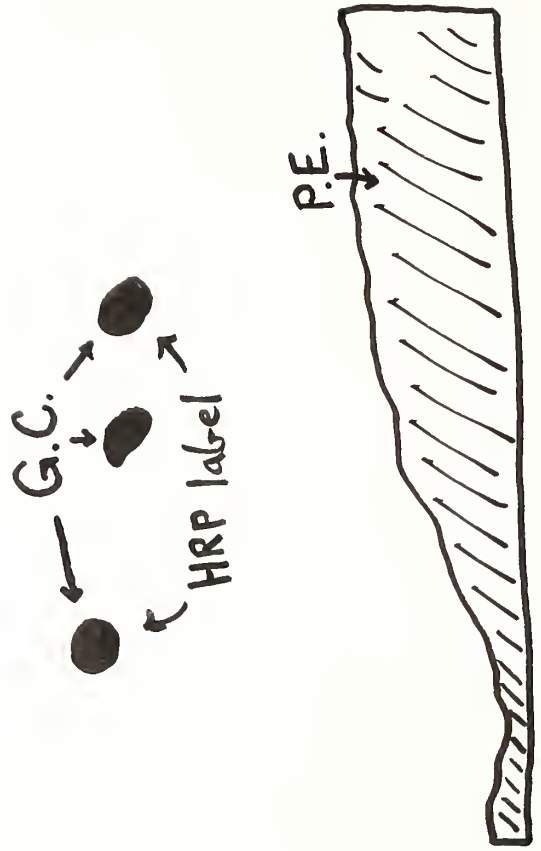

Figure 10B

Fig. 11A. Photomicrograph of a section from the central retina of a Rana pipiens eye showing the ganglion cells retrogradely labeled, following an HRP injection which included LcPt. (Montgomery, et al., 1981).

Figure 11A

Fig. 11B. A schematic of Fig. 11A showing the relative position of HRP-labeled ganglion cells and pigment epithelium (P.E.).

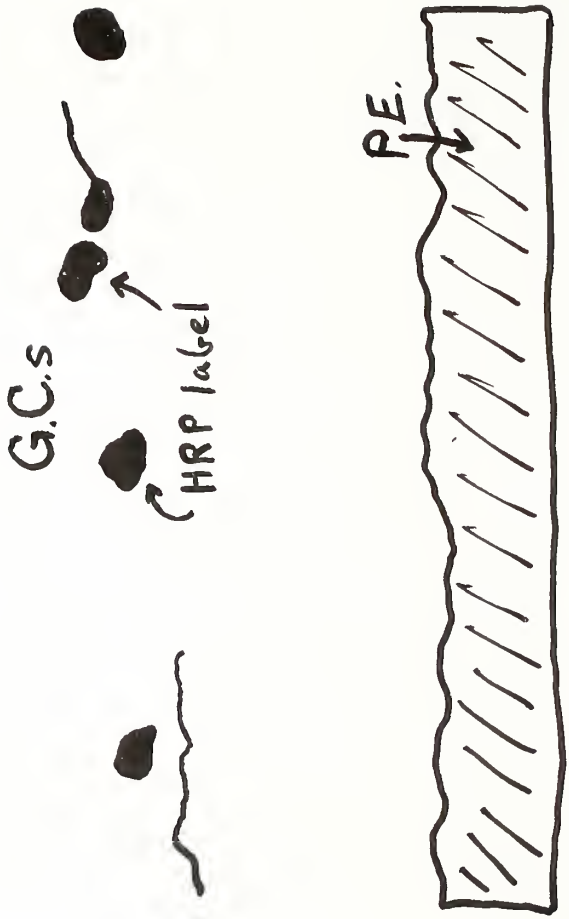

Figure 11B

Fig. 12A. Photomicrograph of a section from the central retina of a Rana pipiens eye showing the ganglion cells retrogradely labeled, following an HRP injection which included LcPt (Montgomery et al., 1981).

Figure 12A

Fig. 12B. A schematic of Fig. 12A showing the position of HRP-labeled ganglion cells and pigment epithelium.

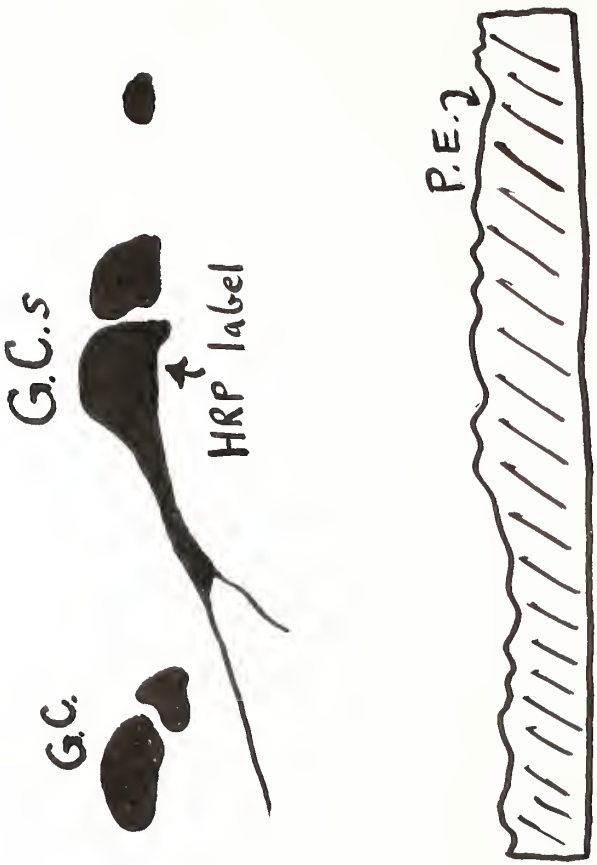

Figure 12B

Fig. 13A. A photomicrograph showing the extent of HRP injection into LcPt (case #33). The plane of section is similar to Fig. 5 (bottom).

Figure 13A

Fig. 13B. A schematic showing the HRP injection site of Fig. 13A and its relation to LcPt, TeO, and Pd.

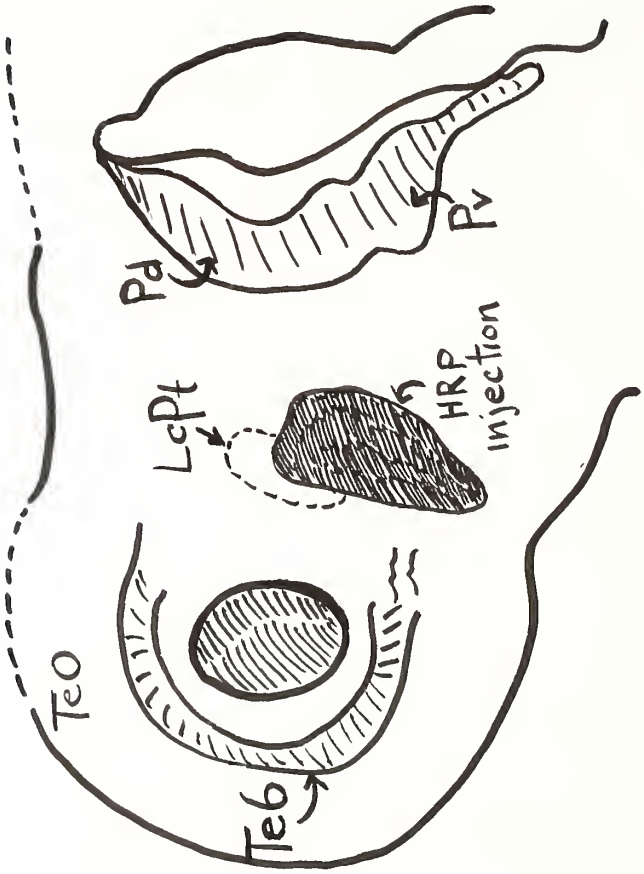

Figure 13B

Fig. 14. A schematic representation of the HRP-labeled ganglion cells in the contralateral eye following a unilateral injection of HRP into LcPt. D - dorsal; V - ventral; N - nasal; T - temporal. Dark spot near the center represents the position of the optic nerve. L - large; M - medium; S - small, (symbols refer to the soma sizes of the HRP-labeled ganglion cells).

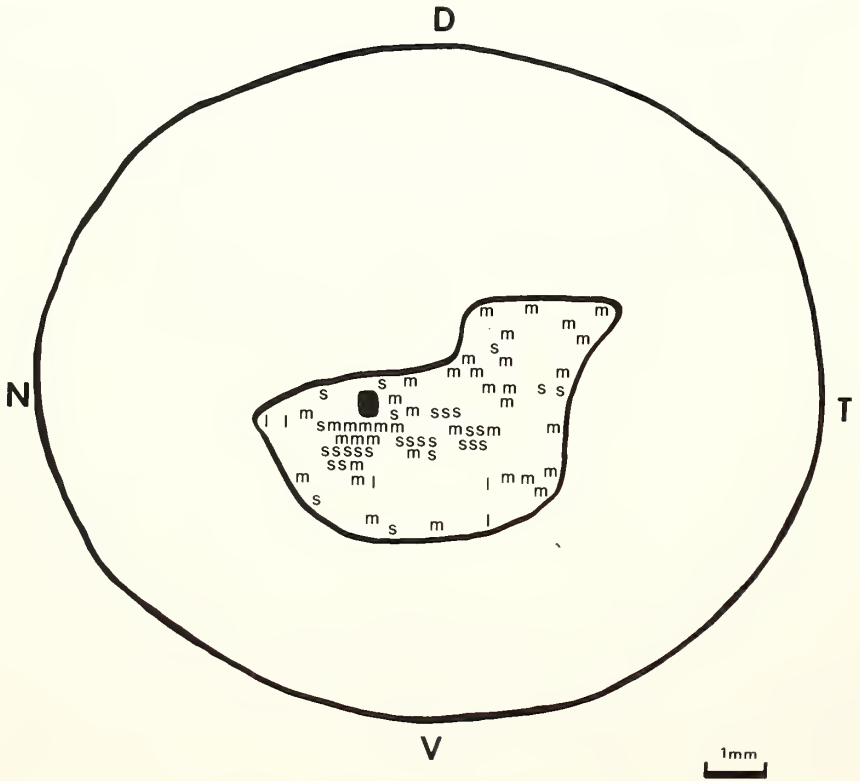
D
N
T
V
1mm

Fig. 15. A reproduction from Carey (1975), showing the regions of greatest ganglion cell density in the retina of Rana pipiens. Note that the shape of this distribution closely approximates the shape of the region of HRP-labeled ganglion cells shown in Fig. 13.

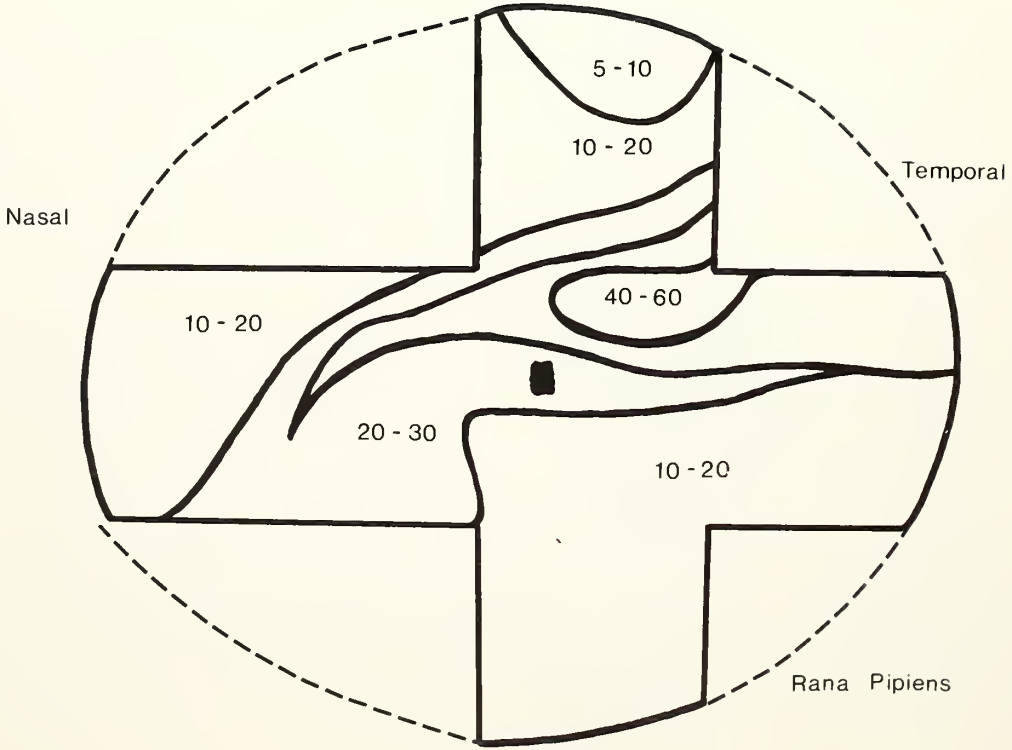
5 - 10
10 - 20
Temporal
Nasal
40 - 60
10 - 20
20 - 30
10 - 20
Rana Pipiens

Fig. 16. A diagram of the entire monocular visual space corresponding to the retina in Fig. 13, showing the region in visual space (the stippled and hatched areas) corresponding to the ganglion cells labeled after HRP injection into LcPt. Stippled area corresponds to a region of greater ganglion cell density. The dotted line represents the total field of view of the HRP-labeled cells, taking into account the receptive field size of the ganglion cells.

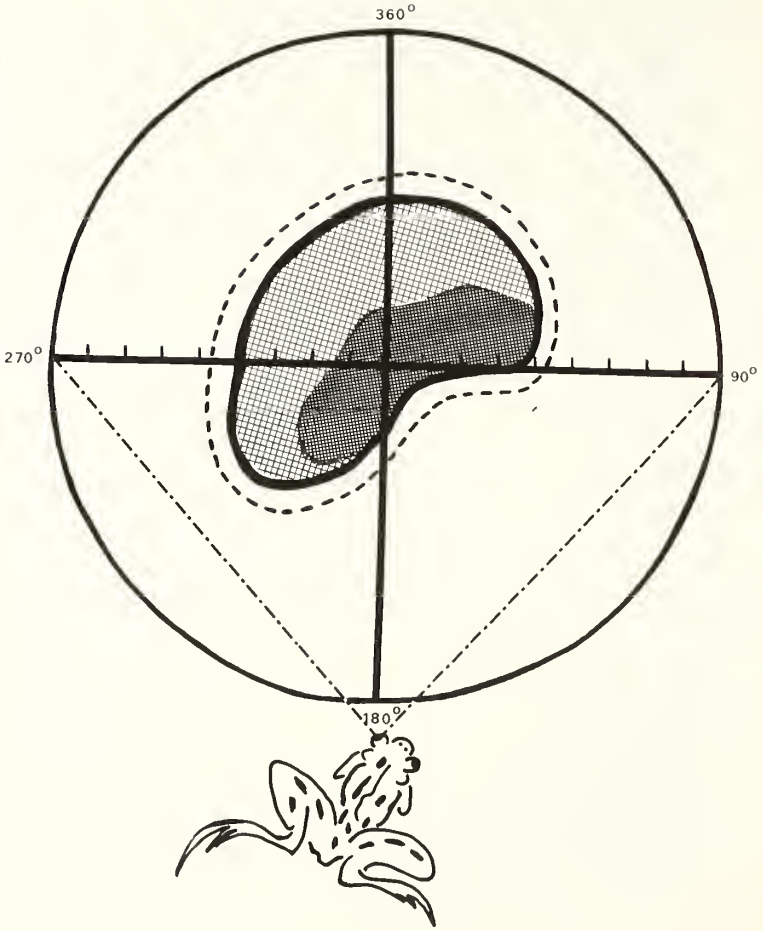
360°
270°
90°
180°

Fig. 17A. Photomicrograph of a coronal section through the pretectal region of Rana pipiens after HRP-optic nerve soak, showing the extent of optic fibers (Montgomery, et al., 1981).

Figure 17A

Fig. 17B. A schematic diagram of Fig. 17A showing the extent of HRP label (hatched area) throughout LcPt, Uncinate, and nBOR, as well as the tectum. Plane of section is similar to Fig. 5 (Bottom).

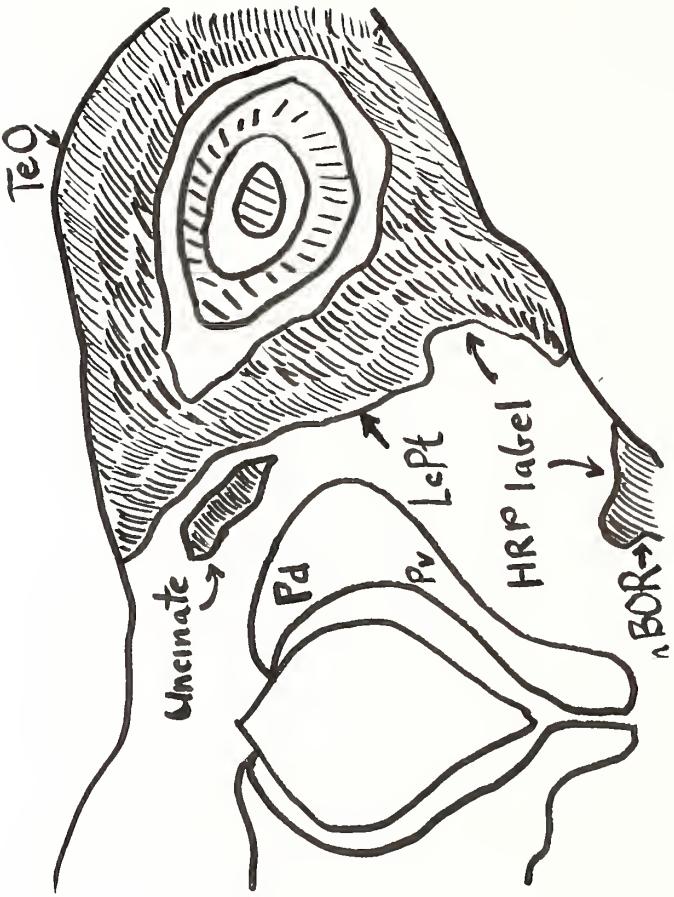

Figure 17B

Fig. 18A. Photomicrograph of the LcPt region following HRP-optic nerve soak.

Figure 18A

Fig. 18B. A schematic of Fig. 18A showing the position of a large cell (arrow) and fibers in LcPt.

Figure 18B

Fig. 19A. Photomicrograph of PtG region showing the extent of the HRP injection site (Montgomery, et al., 1981).

Figure 19A

Fig. 19B. A schematic of Fig. 19A showing the extent of HRP injection site. Plane of section is similar to Fig. 6 (Bottom).

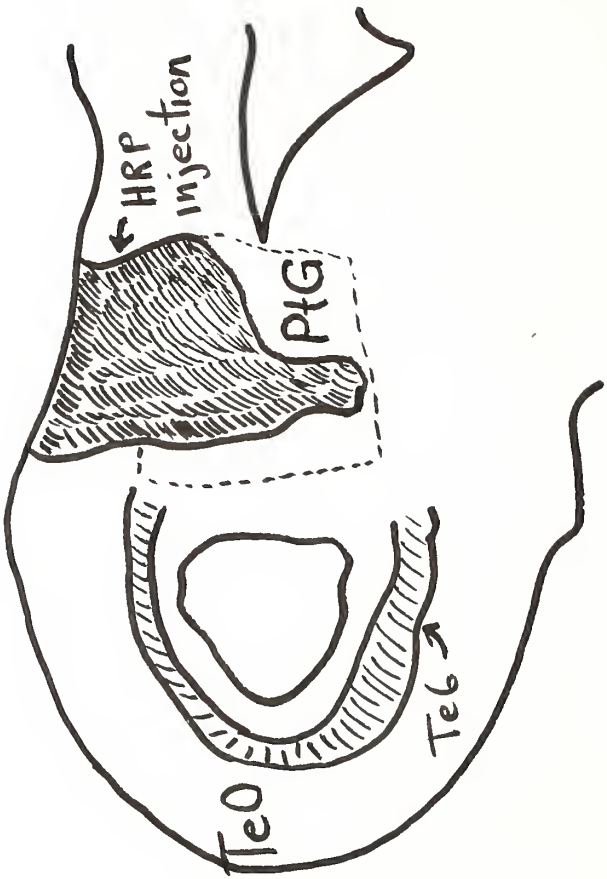

Figure 19B

Fig. 20A. Photomicrograph of LcPt following HRP injection into PtG shown in Fig. 19A. Note the presence of large cells in the dense-core region.

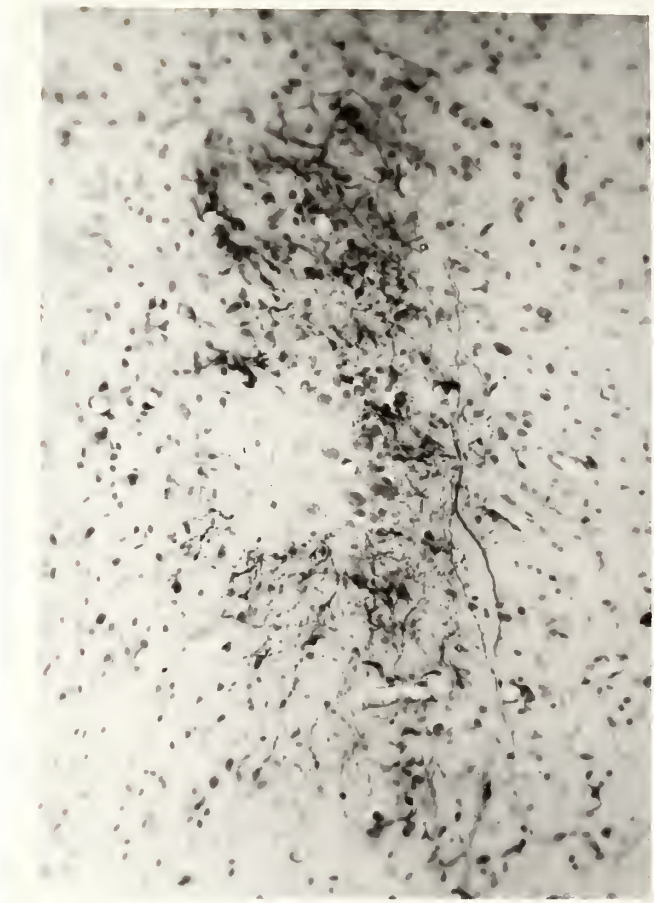

Figure 20A

Fig. 20B. A schematic of Fig. 19A showing the extent of the dense-core region of LcPt. The box represents the extent of Figures 21A and 21B (Montgomery, et al., 1981).

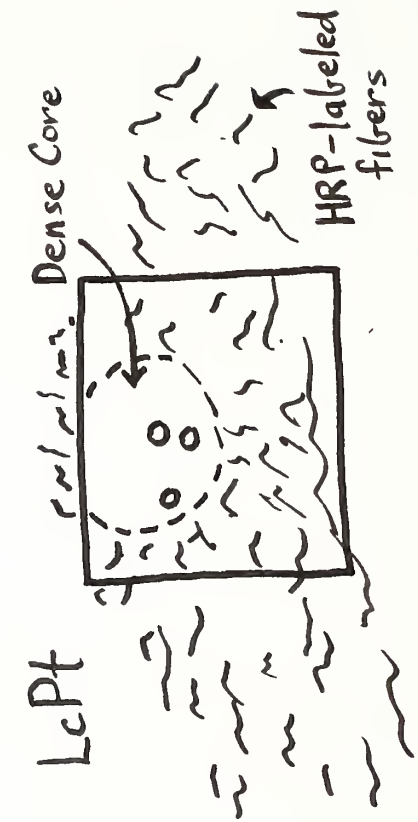

Figure 20B

Fig. 21A. Higher magnification of the region depicted in Fig. 20, showing the termination of fibers outside the dense-core region in LcPt.

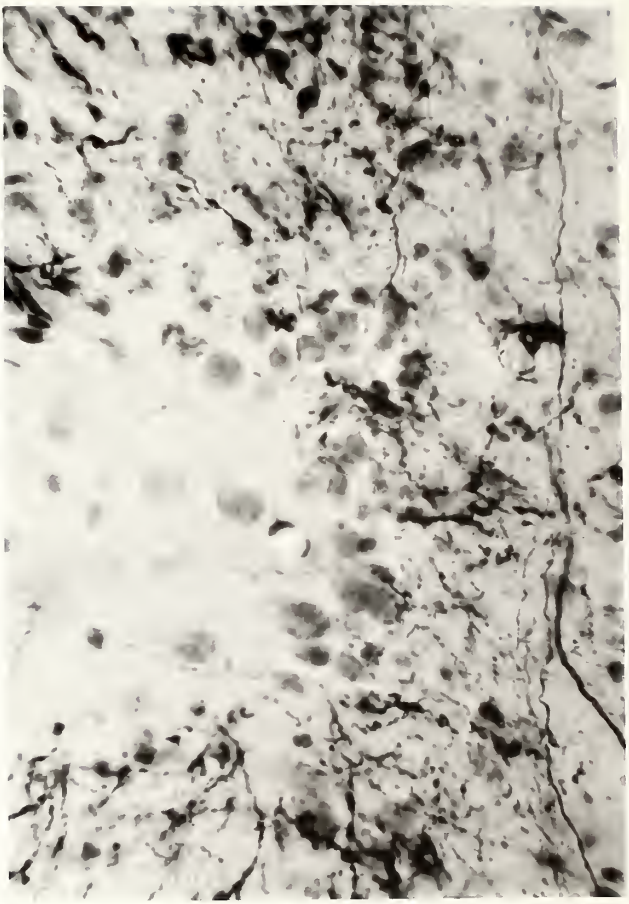

Figure 21A

Fig. 21B. A schematic of Fig. 21A showing the extent of the dense-core region.

Figure 21B

Fig. 22A. Photomicrograph of the nBOR region containing HRP-labeled cells following an HRP injection into LcPt (case #4).

Figure 22A

Fig. 22B. A schematic representation of Fig. 22A showing the positions of HRP-labeled cells in nBOR following HRP injection in LcPt.

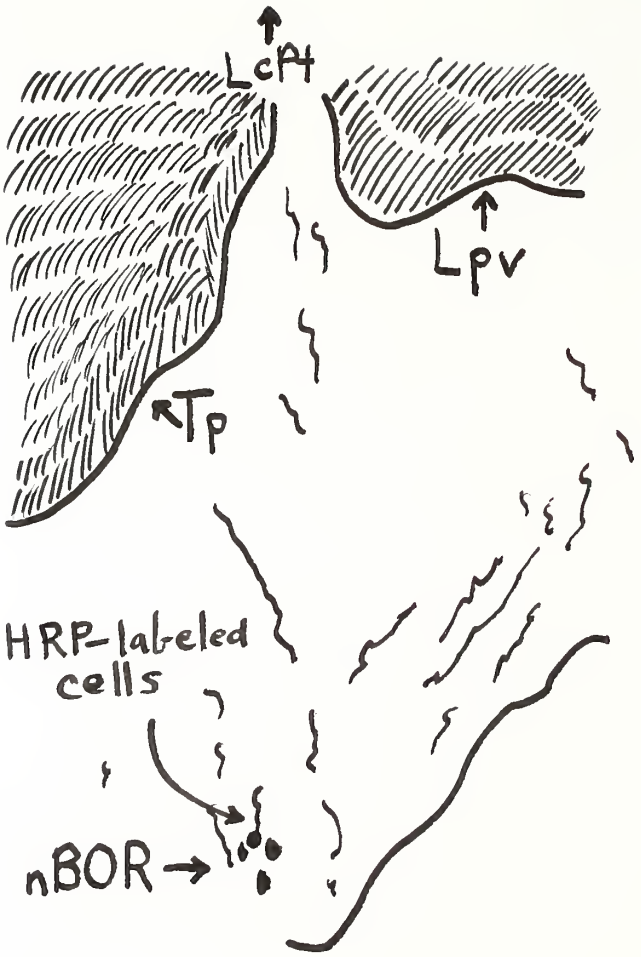

Figure 22B

Fig. 23A. Photomicrograph of the anterior thalamic region containing HRP-labeled cells following injection into LcPt (case #21). The plane of the section is similar to Fig. 4 (Top).

Figure 23A

Fig. 23B. A schematic of Fig. 23A giving the position of HRP-labeled anterior thalamic cells shown in Fig. 23A following HRP injection into LcPt (Case #21).

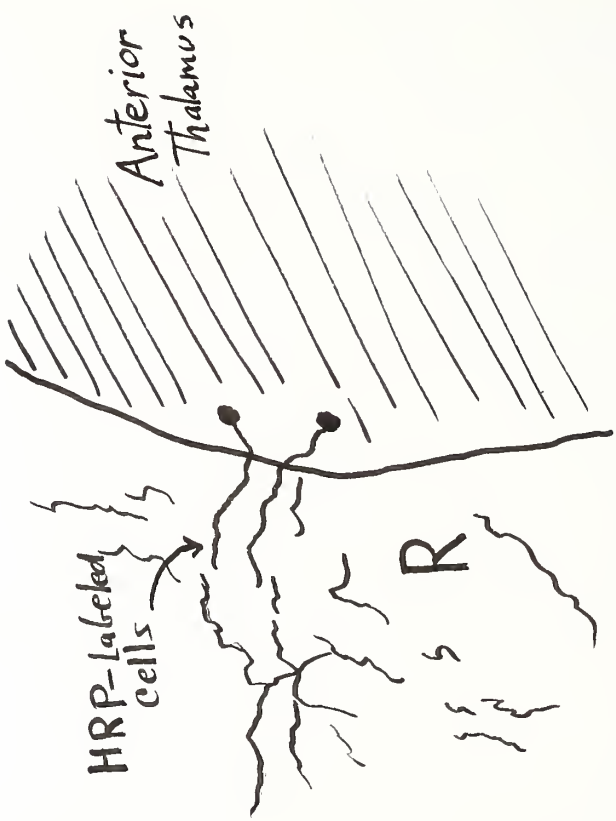

Figure 23B

Fig. 24A. A photomicrograph of a coronal section through the PtG region showing the extent of HRP-labeling following an HRP injection into LcPt (case #21). Plane of section is similar to Fig. 6 (Bottom).

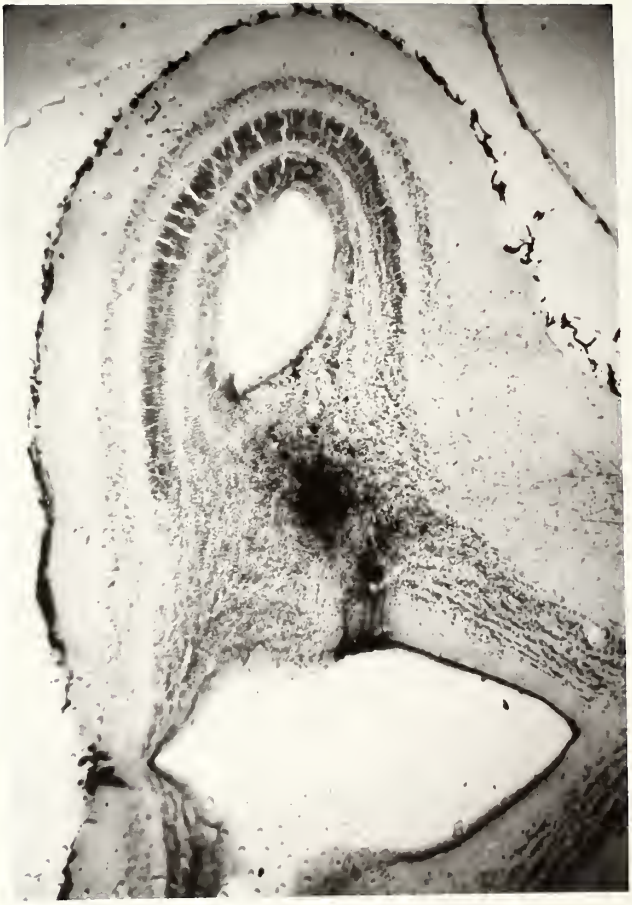

Figure 24A

Fig. 24B. A schematic representation of the PtG region of Fig. 24A, showing retrogradely-labeled HRP cell bodies and fibers. The injection site is shown in Fig. 9.

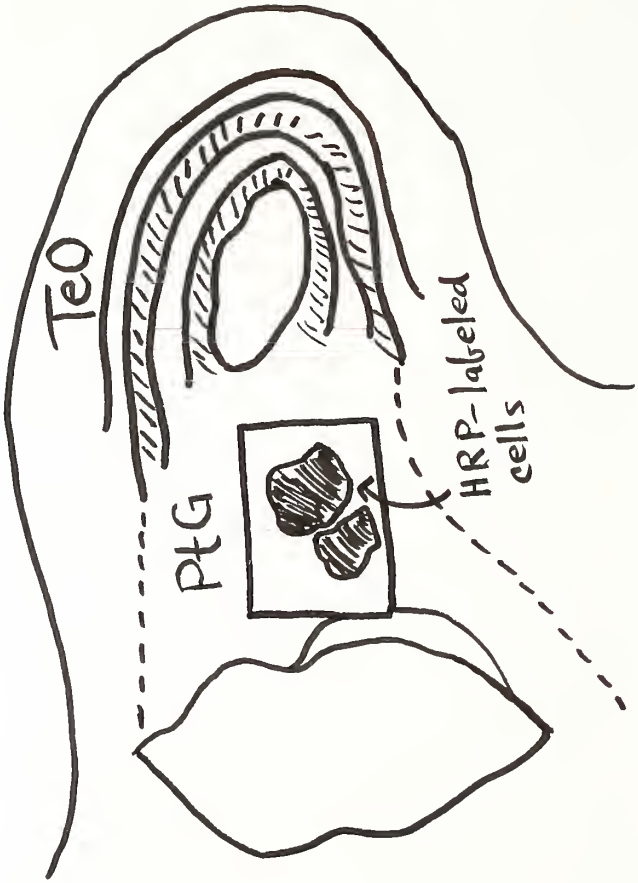

Figure 24B

Fig. 25A. Photomicrograph of the region outlined in Figure 24 B showing the extent of the HRP-labeled cells in PtG following LcPt injection.

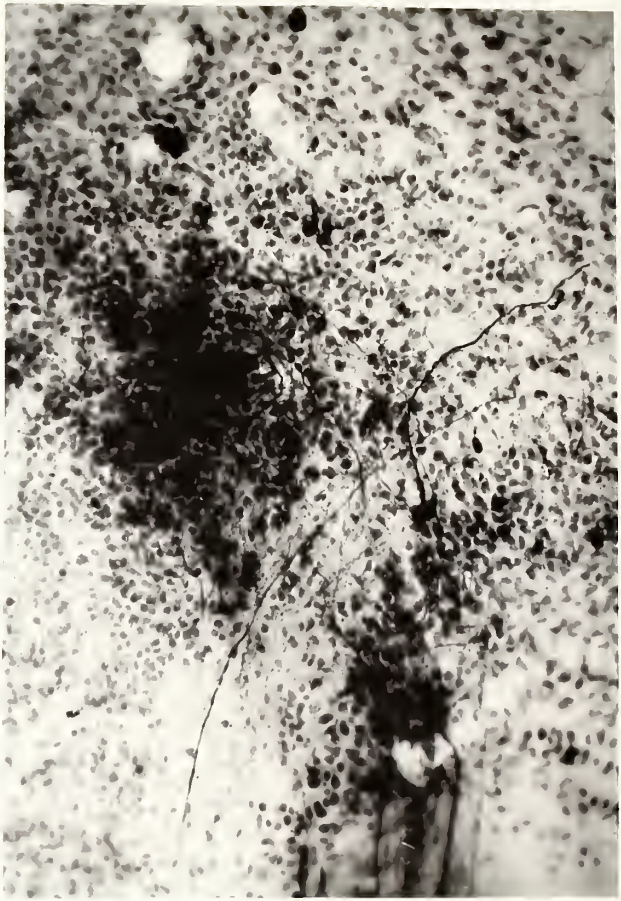

Figure 25A

Fig. 25B. A schematic of Fig. 25A showing the region of HRP-labeling in PtG.

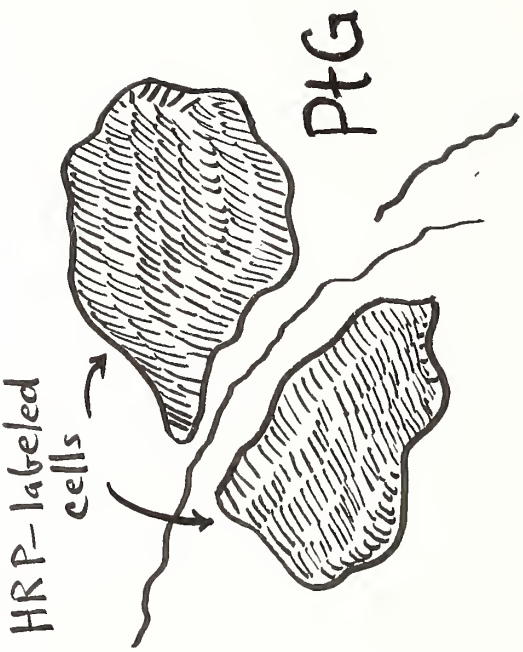

Figure 25B

Fig. 26A. A photomicrograph of a coronal section through LcPt showing the extent of HRP injection (case #18).

Figure 26A

Fig. 26B. A schematic view of the LcPt region shown in Fig. 26A. The plane of the section is similar to Fig. 5 (Bottom).

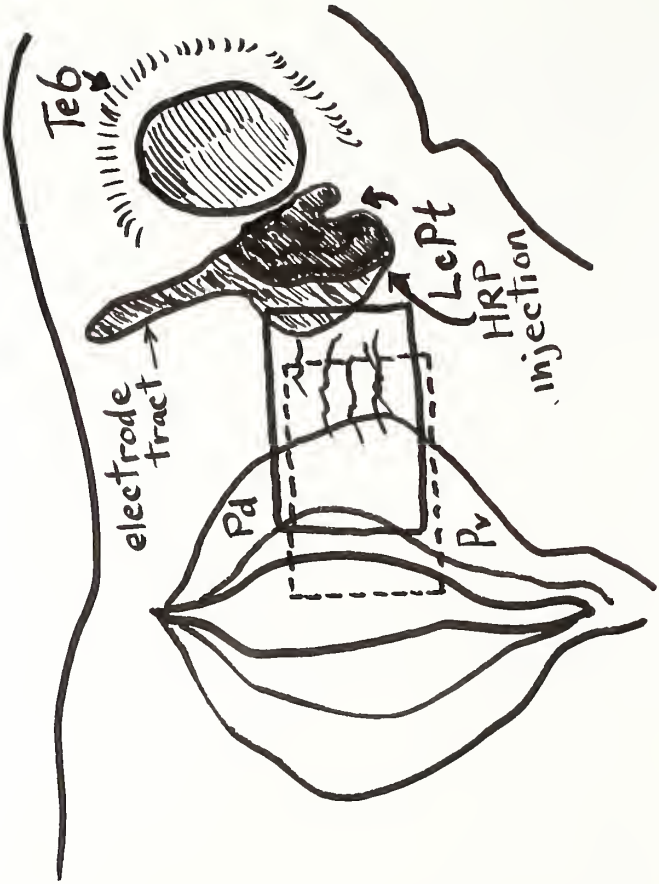

Figure 26B

Fig. 27A. A photomicrograph of the region inside the solid rectangle in Fig. 26B showing the connectivity of LcPt, Lpa and Pv.

Figure 27A

Fig. 27B. A schematic view of Fig. 27A showing the extent of LcPt, Lpd, and Pv.

Figure 27B

Fig. 28A. A photomicrograph of the Pv and Lpd regions within the dotted rectangle shown in Fig. 26B.

Figure 28A

Fig. 28B. A schematic view of Fig. 28A showing the extent of Lpd and Pv.

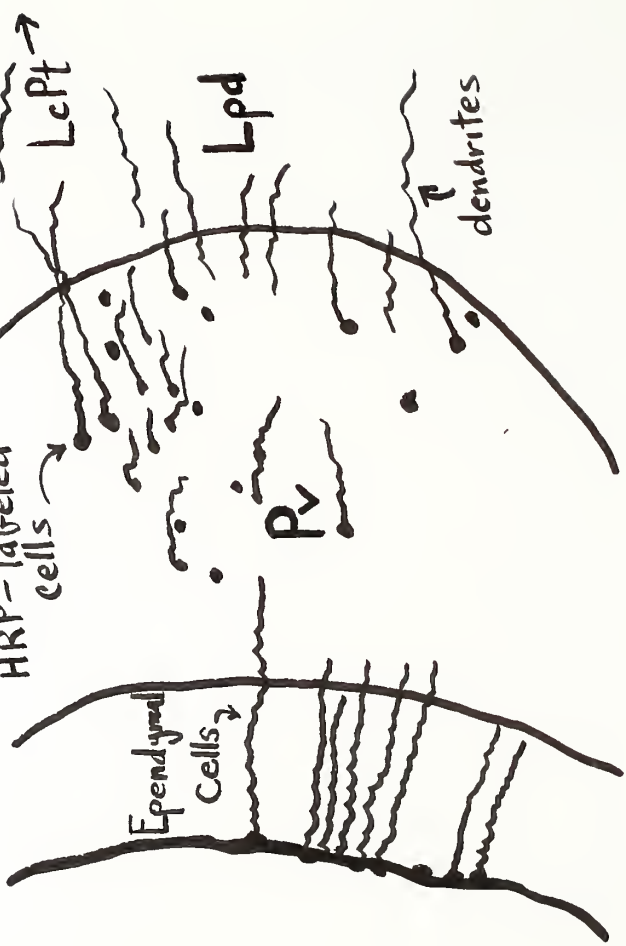

Figure 28B

Fig. 29A. A photomicrograph of a coronal section through the pretectal region of Rana pipiens showing the site of an electrolytic lesion following unit recording in LcPt (#13).

Figure 29A

Fig. 29B. A schematic representation of the electrolytic lesion shown in Fig. 29A showing its relation to LcPt and TeO.

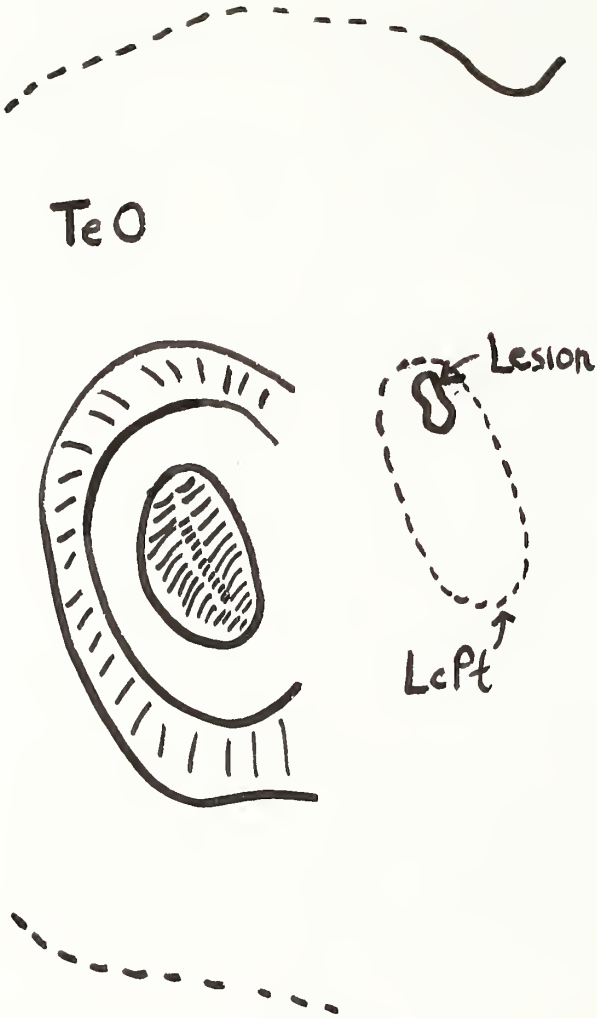

Figure 29B

Fig. 30A. A photomicrograph of a coronal section through the pretectal region in Rana pipiens showing the extent of an electrolytic lesion following unit recording in LcPt (#14).

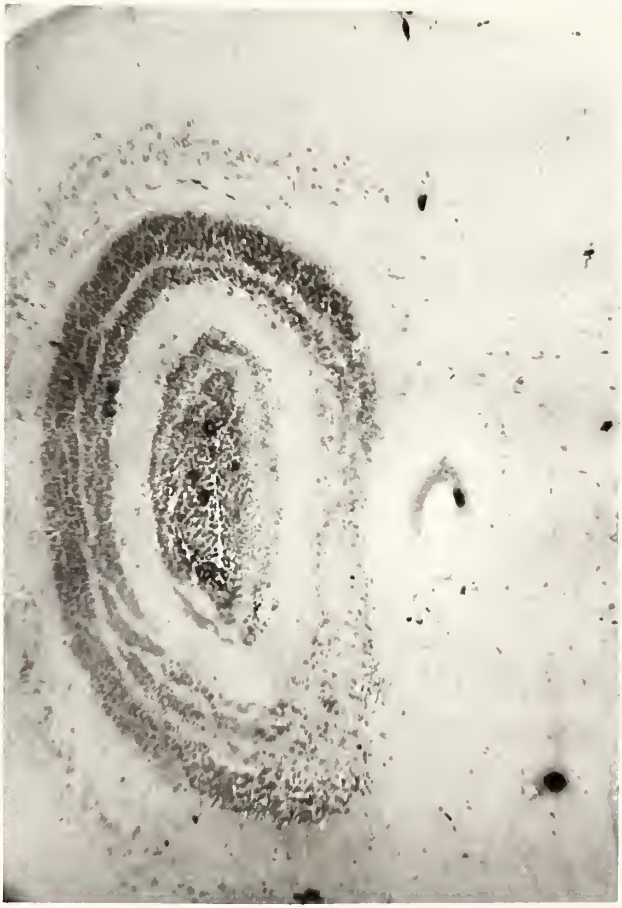

Figure 30A

Fig. 30B. A schematic of Fig. 30A showing the electrolytic lesion site and its relation to LcPt and TeO.

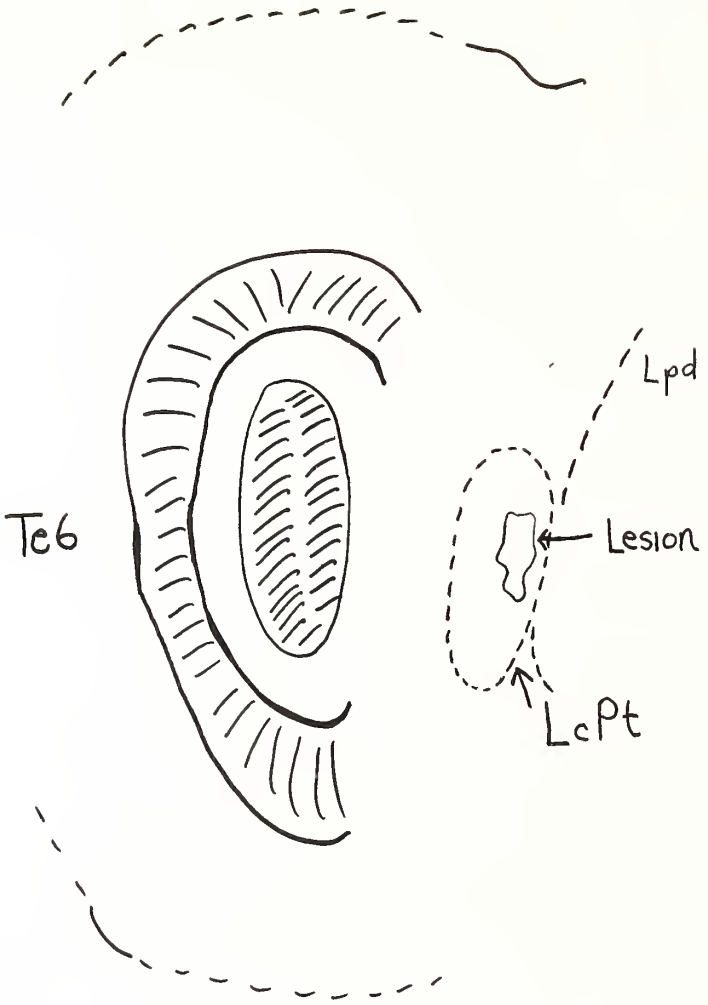

Figure 30B

Fig. 31. A schematic diagram of coronal sections through the meso-diencephalic region in Rana pipiens showing the electrolytic lesion sites following single unit recording in the pretectal and surrounding regions. Inset shows a lateral view of Rana pipiens brain with the coronal sections indicated in cross-section. (LOT) Lateral optic tract; (MOT) Marginal optic tract. The shaded areas represent densest regions of cell bodies.

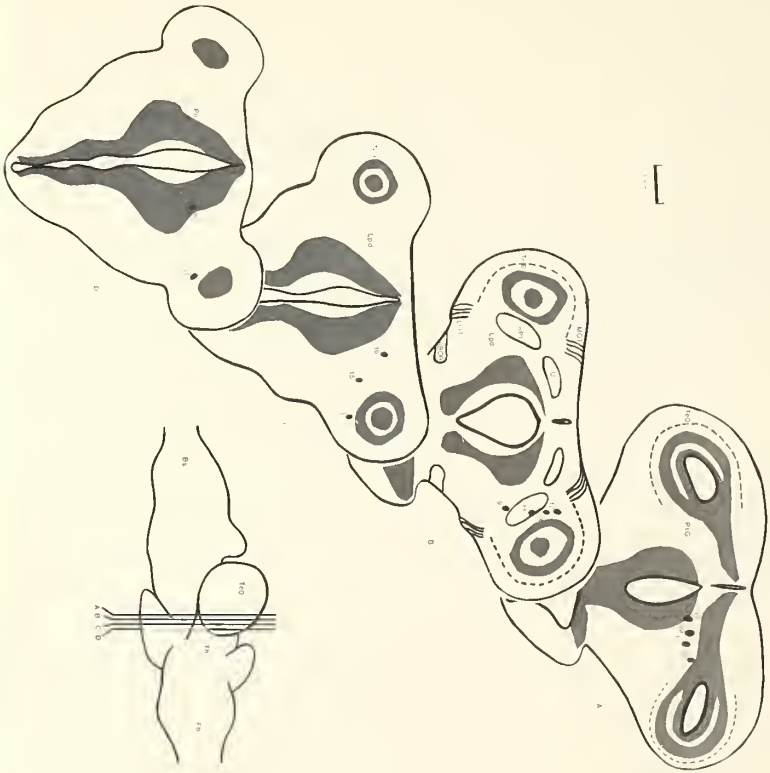
PIG
THO

Fig. 32. A: High speed spike record from unit #14 in LcPt. Negative = up.
B: Same as 'A' for unit #13 in LcPt.
C: Same as 'A' for unit #16 in Lpd.
D: Response of unit #14 to onset of horizontal OKN stimulus movement (arrow).
E: Response of unit #17 in PtG to onset of horizontal OKN stimulus movement (arrow), from right to left, at 15°/sec.

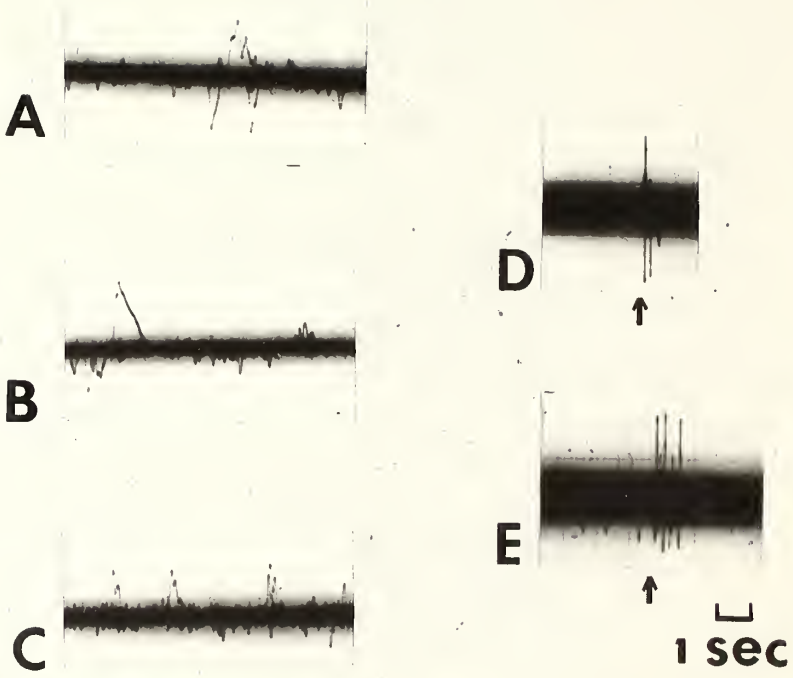
A
B
C
D
E
1 sec

Fig. 33. A: Spontaneous activity of unit #19 (in PtG) in the dark.
B: Same unit as in 'A' during slow (10°/sec.) horizontal OKN stimulation in the nasal-temporal direction.
C: Same unit as above after onset of a large shadow (arrow) moving in the dorsal-ventral direction.

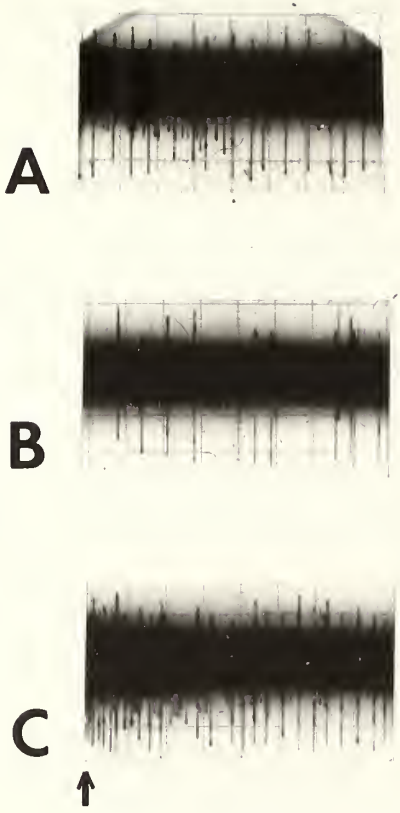
A
B
C
2 sec

Fig. 34. A: Spontaneous activity of unit #18 (in PtG) in the dark.
B: Same unit after light onset (left arrow) and light offset (right arrow).
C: Same unit in the presence of stationary horizontal OKN stimulus.
D: Same unit during slow (10°/sec.) movement of horizontal OKN stimulus in the nasal-temporal direction.

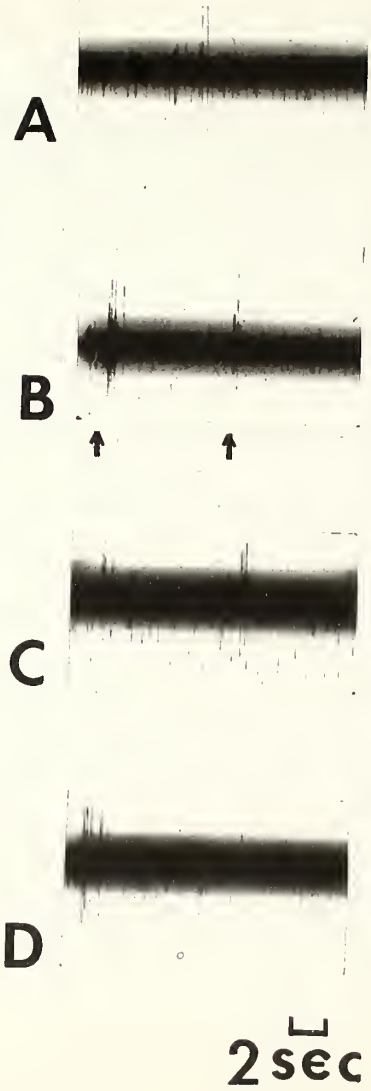
A
B
C
D
2 sec

Fig. 35A. A photomicrograph of a coronal section through the region anterior to LcPt in Rana pipiens showing the location of an electrolytic lesion following unit recording from Lpd (#16A).

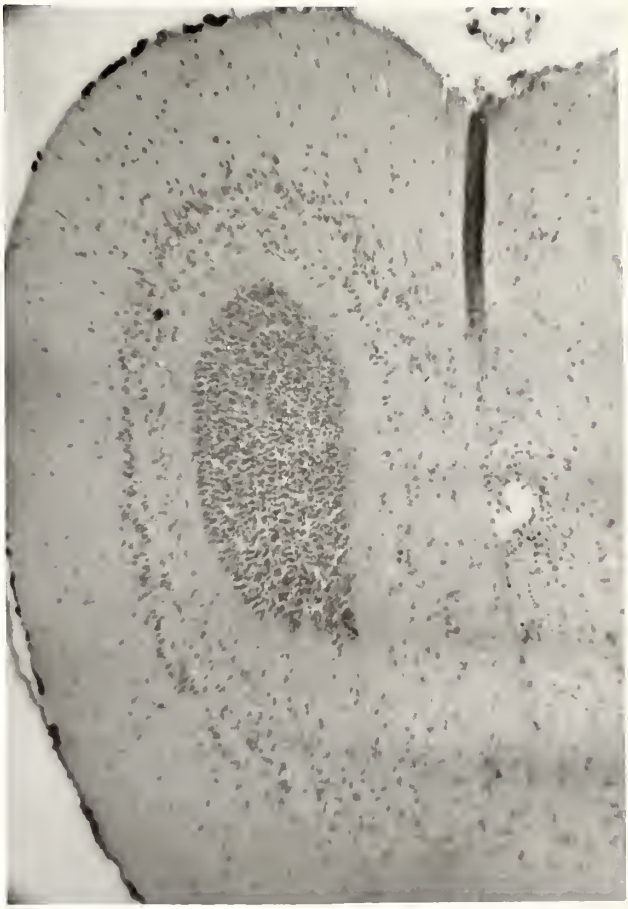

Figure 35A

Fig. 35B. A schematic representation of the region shown in Fig. 35A showing the relation between the electrolytic lesion and Lpd and TeO.

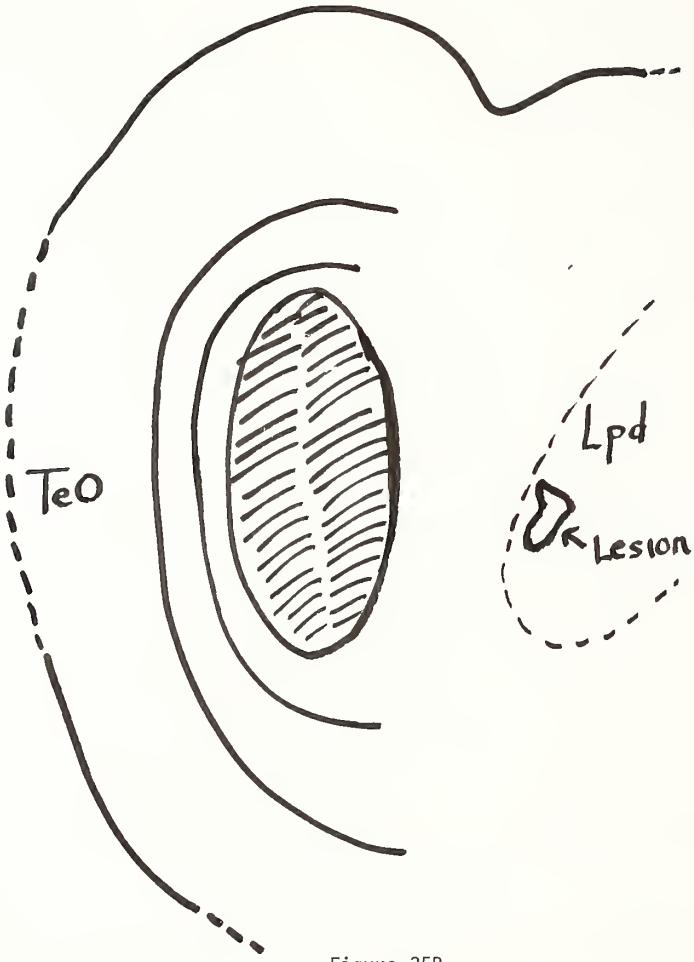

Figure 35B

Fig. 36. A schematic representation of the interconnections between LcPt and other brain regions. For nomenclature, see Table I.

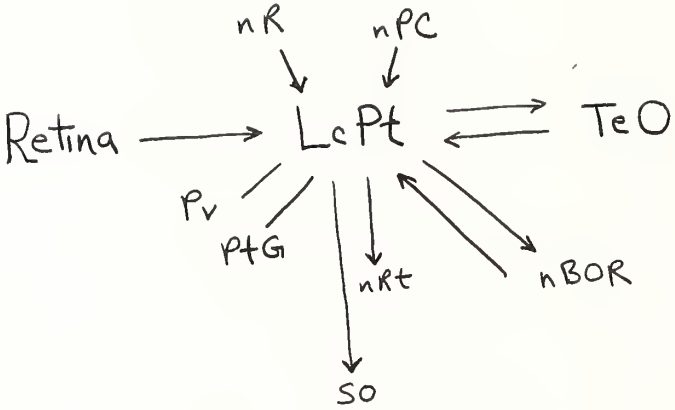

Figure 36